GTI 5G Device OTA Performance White Paper

http://www.gtigroup.org

GTI 5G Device OTA Performance White Paper

Version:	V1.0
Deliverable Type	□ **Procedural Document** √ **Working Document**
Confidential Level	√ **Open to GTI Operator Members** √ **Open to GTI Partners** □ **Open to Public**
Program	5G eMBB
Working Group	Terminal WG
Project	Project 5: Test Equipment
Task	5G Device OTA Task Force
Source members	Anritsu, Bluetest, China Mobile, GeneralTest, Huawei, Hwa-tech, Keysight, OPPO, Qualcomm, R&S, RTC, Sunway, Smartisan
Support members	Xiaomi, Samsung, vivo, Simcom, Starpoint

Editor	Hao Hu, Honggang Sui, Yifan Liu, Zheng Zhang, Meng Hou, Yujuan Ma, Ya Jing, Jinqiang Xing, Bin Han, Sijia Gu, Yueting Cai, Qing Xu, Tao Liu, Anmin Xu
Last Edit Date	21-01-2019
Approval Date	DD-MM-2019

Document History

Date	Meeting #	Version #	Revision Contents
DD-02-2019	24nd GTI Workshop	V1.0	The first version of GTI 5G device OTA performance white paper. The antenna design, OTA performance analyses and test methods for Sub-6G and mmWave 5G devices are described.

Table of Contents

1 Executive Summary

This white paper provides a technical overview of the **5G device OTA performance**. As we all known, OTA is the key method to evaluate the antenna performance and the OTA performance of wireless devices and reflect its access and throughput performance in real network.

Antennas are key component of wireless devices and directly determine the OTA performance of 5G devices. With the pursuit of aesthetic and complex functions and architectures, it is hard to provide antennas good operating environment which result in the decrease of antenna performance. What we can do to improve the performance of antennas need to be discussed.

Sub-6G devices have 2Tx and 4Rx transmit and receive character. With more antennas, the radiative and sensitivity performance of Sub-6G devices would be better and they can benefit from not only downlink but also uplink MIMO. The OTA performance are determined by many factors, such as the chipset capability, the antenna performance, the interference and the match problems. In order to make sure that the 5G devices be able to benefit from the beamforming gain and satisfy the network requirement, the OTA performance requirements are necessary. However, the UL MIMO performance has never been discussed before and this task force also take the responsibility to bring the industry attention to finding out the solutions for 5G device UL MIMO performance.

mmWave devices usually have highly integrated architectures so they may not be able to physically expose a front-end cable connector to the test equipment. Then OTA is the main test methodology for mmWave 5G devices. Not only radiative and throughput performance, but also protocol, RF and RRM conformance tests will adopt OTA solutions and the research on this area is brand new for the industry.

What's more, transmit and receive status is different for NSA and SA 5G devices. So the radiative and MIMO performance requirements should differ with implementation and the influence of LTE link should be also taken into consideration.

In general, OTA performance is quite important to make sure that 5G devices operate at high-performance in real network. This task will focus on studying the OTA performance of 5G devices and discuss the available test solutions.

2 Abbreviations

Abbreviation	Explanation
3GPP	3rd Generation Partnership Project
AAS	Active Antenna System
AS	Angular Spread
CE	Channel Emulation
ECC	Envelope Correlation Coefficient
eMBB	enhanced Mobile Broad Band
E-UTRA	Evolved Universal Terrestrial Radio Access
FCC	Federal Communications Commission
FHD	FraunHofer Distance
GTI	Global TD-LTE Initiative
IFF	Indirect Far Field
IMT	International Mobile Telecommunication
ITU	International Telecommunication Union
ITU-R	International Telecommunication Union - Radio
LCP	Liquid Crystal Polymer
LNA	Low Noise Amplifier
LTE	Long Term Evolution
mMTC	massive Machine Type Communications
MPAC	Multi-Probe Anechoic Chamber
MPI	Modified Polyimide
NR	New Radio
RAN	Radio Access Network
RC	Reverberation Chamber
RF	Radio Frequency
RMC	Reference Measurement Channel
SCME	Spatial Channel Model Extension
SDL	Supplementary Downlink
SDO	Suspect Disturbing Objects
SG	Signal Generator
SUL	Supplementary Uplink
TDD	Time Division Duplex
TDL	Tapped Delay Line
TD-LTE	Time Division Long Term Evolution
TRP	Total Radiated Power

TRS	Total Radiated Sensivity
uRLLC	ultra-Reliable and Low Latency Communications
VSWR	Voltage Standing Wave Ratio

3 Introduction

To get fully prepared before the commercialization in 2020, China mobile planned 3 phases of validation of 5G, namely, the key technology test, the system test and the large-scale test. The key technology test and the system test have been completed separately in 2016 and 2017 and now the validation has proceed to phase three. The large-scale test includes two parts: the trial test and the laboratory test. Both of the two parts will be carried out in parallel. OTA test is an important component in laboratory test and mainly focuses on the function and the performance validation of 5G devices.

5G has hold out high requirements to devices which bring great challenges to OTA test. For Sub-6G bands, it is mandatory to support 2Tx and 4Rx antenna structure, which means we need to extend the 2x2 to 4x4 MIMO in downlink and explore new solution for uplink MIMO measurement. What's more, not only azimuth but also elevation angles are needed therefore much more probes are need. For mmWave bands, the antenna is such highly integrated that there is no way to connect device with a cable and then only the wireless link can be used. So we also need to explore OTA method to carry out all the test, such as the RF, RRM and demodulation performance test.

Being faced with so many challenges, GTI 5G device OTA group leads to write the "GTI Device OTA performance White Paper". This whitepaper is expected to attract people's attention to OTA performance evaluation of 5G devices, analyses OTA performance requirements and find suitable test solutions. Hope this whitepaper can give a guidance to the industry for antenna design and quality control. This is the first version of white paper and we introduced the antenna design principles, the OTA performance requirements and the potential test solutions for 5G devices. Since the antennas forms, performance and test methods are quite different between FR1 and FR2, all the analyses are carried out separately for Sub-6G and mmWave devices.

4 Sub-6G Device Antenna

4.1 Introduction

There are 3 typical scenarios for 5G application: eMBB (enhanced mobile broadband)，uRLLC (ultra-reliable and low latency communications) and mMTC (massive machine type communications). URLLC and mMTC are mainly implemented by 5G protocol layer. Aiming at Gbps data rate eMBB requires the synchronization optimization between hardware and protocol layer. In order to achieve this goal, the following RF applications will be applied for 5G network and devices:

- Advanced MIMO
- Wider carrier bandwidth
- High frequency carrier

Among them, 2 and 3 involve carrier frequency redistribution. Compared with LTE network, 5G needs broader spectrum and higher frequency carrier to achieve Gbps data rate. 3GPP combed the current spectrum resources and defined the spectrum used by 5G. For the frequency bands lower than 6 GHz (FR1), it is called sub 6GHz bands; for those higher frequency range (FR2), generally it is called mm-Wave bands. As shown in Table 4-1

Table 4-1 5G frequency range

Frequency range	Corresponding frequency range
FR1	450 MHz – 6000 MHz
FR2	24250 MHz – 52600 MHz

The maximum bandwidth is 100MHz for sub-6GHz is and 400MHz for mm-Wave. 15KHz and 30 KHz subcarrier spacing can be used only in Sub 6 GHz and 120 KHz subcarrier spacing can be used in mm-Wave range only. 60 KHz subcarrier spacing can be used both in sub-6G and mm-Wave range. According to Shannon's law, it is obvious that the use of millimeter wave is more conducive to achieving high data rate, but sub 6GHz spectrum has better coverage and mature optional components. The use of sub 6GHz RF front-end will be more conducive to the initial deployment of 5G. So we need to pay more attention to the application of sub 6GHz at present. The defined sub 6GHz band resources are shown in Table 4-2.

The available band resources of 5G are all named after the letter “n”, which represent “new radio”. The supplementary band of sub-6G is introduced in the Table 4-2, which can improve the coverage of the high frequency. It can be combined with the high frequency by carrier aggregation or dual connection.

Table 4-2 Frequency Band in Sub 6GHz

FR1

Band	Uplink	Downlink（MHz）	Bandwidth（MHz）	Duplex
n1	1920~1980	2110~2170	60	FDD
n2	1850~1910	1930~1990	60	FDD
n3	1710~1785	1805~1880	75	FDD
n5	824~849	869~894	25	FDD
n7	2500~2570	2620~2690	70	FDD
n8	880~915	925~960	35	FDD
n20	832~862	791~821	30	FDD
n28	703~748	758~803	45	FDD
n38	2570~2620	2570~2620	50	TDD
n41	2496~2690	2496~2690	194	TDD
n50	1432~1517	1432~1517	85	TDD
n51	1427~1432	1427~1432	5	TDD
n66	1710~1780	2110~2200	70/90	FDD
n70	1695~1710	1995~2020	15/25	FDD
n71	663~698	617~652	35	FDD
n74	1427~1470	1475~1518	43	FDD
n75	NA	1432~1517	85	SDL
n76	NA	1427~1432	5	SDL
n77	3300~4200	3300~4200	900	TDD
n78	3300~3800	3300~3800	500	TDD
n79	4400~5000	4400~5000	600	TDD
n80	1710~1785	NA	75	SUL
n81	880~915	NA	35	SUL
n82	832~862	NA	30	SUL
n83	703~748	NA	45	SUL
n84	1920~1980	NA	60	SUL

5G antenna technologies are playing a very important role for 5G applications. It should have the following features:

- More independent antennas, polarized antennas
- Multi-spectral coexistence, not use time sharing tuning in a band
- High gain

Compared with mm-Wave bands, bandwidth of sub 6GHz is not big enough so the more antennas should be used to achieve higher data rate. 5G Sub-6G devices are mandated to have 4 antennas for downlink and 2 antennas for uplink. Compared with 4G devices, the number of antenna is doubled and brings great challenges for antenna design. In order to support all the 5G bands, devices applied to 5G network need have more than four antenna ports simultaneously. The implementation technology would be multiple antennas or multiple feeders in one antenna. The antenna with orthogonal polarizing ports, such as horizontal polarization and vertical polarization. When the two ports have good isolation, also can be

used for MIMO and full duplex.

Design the antenna used in 5G network device, the lump-elements that are applied to antenna's impedance tuning need to be more carefully selected. The element numerical precision, self-resonant, Q value also need to be concerned. The harmonic characteristics of the active tuners (switch and adjustable capacitance) need special attention.

The radiation efficiency of the antenna need to improve. The antenna radiation characteristics can be controlled by designing the surface current distribution and boundary environment of antenna structure.

4.2 Antenna Design philosophy and principle

Antenna is passive microwave device, obey the law of conservation of energy. The antenna can be considered as an energy exchange device and the primary task is to achieve minimum loss. The antenna can be considered as a bridge between electric circuit and electric field. In circuit domain, similar to filter, passband performance needs to be well designed. In field domain, similar to airspace filter, radiation pattern needs to be well designed.

Antenna is a typical asymmetric two-port network, which usually use VSWR to describe the performance of the RF connection port and radiation pattern to describe the performance of the external connection port (usually free space).

Usually, impedance matching network is used to obtain good VSWR, which should realize minimum loss and control the harmonic characteristic. The implementation method on the mobile phone is consistent with existing phone which support CA. Radiation efficiency is used to describe the performance of space connection. The antenna can be considered as a distributed circuit, which can be described in formula 4-1. For the same type of antenna, the product of its bandwidth and radiation efficiency is proportional to the antenna's space. In order to compare different frequency bands, we can use relative bandwidth instead of B, and electrical size (the number of wavelength) instead of V. Now the antennas of smartphones are all built in, and under the same antenna's space, the monopole has biggest product of bandwidth and radiation efficiency.

$$B*\eta \propto V \tag{4-1}$$

where：

B: antenna bandwidth

η: radiation efficiency

V: the space of antenna, include the antenna structure and the boundary space

In the actual project, it is difficult to obtain the exact value of V, but formula 4-1 still can be used to measure the limit state of antenna's passband design. For example, an antenna is designed under the condition of the whole machine, and the efficiency bandwidth of the

antenna can be obtained. It can be predicted that in order to improve the efficiency, the bandwidth can be reduced or the efficiency can be reduced to expand the bandwidth. It can also be used to determine whether the time-sharing tuner is needed.

How to improve the efficiency of antenna radiation，in a word，carefully deal with the antenna boundary. From an energy perspective, the antenna boundary is roughly divided into two types, energy loss type and energy storage type. The energy loss is mainly the dielectric loss of the materials around the antenna，such as plastic and coating. We should choose the material with small loss tangent.

For current cellule operating bands, such as LTE band 7 (2500---2690MHz), 41 (2496---2690MHz), and band 22 in Japan (3410---3590MHz), operates at similar frequency range as Sub-6G bands (n41: 2496---2690 MHz, n78: 3300---3800MHz, and n79: 4400---5000 MHz)

If the CMF (colour, materials, and finishing) design of the Sub-6G devices is similar as LTE devices', and the electrical parameters of materials that impact antenna performance, such as permittivity and loss tangents, will be not much different. The common materials have already been verified for antenna design in LTE devices. The antenna radiator and substrate should be also similar.

Currently, the conventional materials and radiators of antenna element are shown as following

- On metal frame
- Metal plating on plastic: LDS, PDS
- Flex film radiator

Antenna substrate material, such as pc, abs, are still well used. Some novel low loss materials, like LCP (Liquid Crystal Polymer) and MPI (modified polyimide) were investigated and applied in the devices. Still the basic antenna element design concepts are expected to be not big different between of sub 6GHz phones and 4G LTE phones.

Another thing that should be considered for antenna design is to reduce energy storage. The main way is to reduce capacitance. Smartphone is very compact, there are metal material components nearby the built-in antenna, such as speaker, USB bridge, shielding can, camera, vibrator, etc. There will be plate capacitance effect between these components and antenna body. We use the formula of plate capacitance formula (4-2) to analyse this problem. If we want to reduce the capacitance, we need to decrease the area S and distance d. In antenna design, we should to increase the distance between the component and the antenna body and reduce its surface area parallel to the antenna body. If there are multiple components, the effect is equivalent to capacitance parallel. Priority should be given to the one which nearby the antenna current device. Since the antenna is a current excitation, its device has high voltage.

$$C = \varepsilon \cdot \frac{S}{d} \tag{4-2}$$

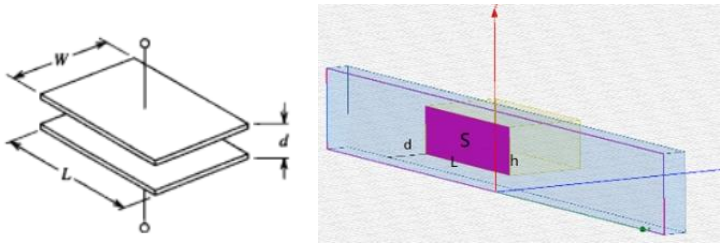

Figure 4-1 Capacitance Structure

The antenna radiation pattern is mainly described as the energy distribution in the 4π spheres wrapped around the antenna structure (with the antenna phase centre as the spherical centre). From the radiation principle, the radiation pattern of the antenna is determined by the surface current distribution of the antenna structure. Therefore, we can design the antenna surface shape to achieve the expected radiation pattern and polarization. We know the direction of the energy transfer from electromagnetic waves is the cross product of electric field and magnetic field. Both electric field and magnetic field are vector fields, and they are always orthogonal. We use the direction of the electric field defined as the electromagnetic field vector.

Furthermore, 5G communication system need multiple RF paths, which are used for MIMO application. Accordingly, multiple independent antenna ports or antennas are required.

How to design a good antenna system used in MIMO communication. First, antennas should have good individual performance, then an antenna need to be independent from other antenna, which usually measured by correlation index. In the scheme, orthogonal dual-polarization antenna and space layout multi-antenna can be used. It is difficult to implement orthogonal dual-polarization antenna in smartphone. But it can design a spatial antenna system in smartphone, also used the concept of the polarization to improve correlation index.

We describe the basic principle of MIMO system antenna's design by taking two antennas for example. In stadia condition, the transmission properties of electromagnetic wave can be similar to optics line. If you had two flashlights in the dark space, what would you do to illuminate more space? Usually, the flashlights are located at a distance or at an angle (shown in Figure 4-2). Multiple antenna design applies the same scheme to realize the independent transmission path of stadia. Due to the limited physical size of smartphones, it is difficult to put antennas in ideal distance. Also, we can use the included angle and polarization to improve the correlation index. In general, the distance between two antennas needs to be more than half-wavelength, the linear current vector distribution of two antennas are orthogonal.

Figure 4-2 Multiple Lights in Darkness

For example, we can use the following multi-antenna layout (Figure 4-3) to achieve better MIMO performance. There is maximum space between antenna_1 and antenna_2. Antenna_3 and antenna_4 use the different antenna shapes to achieve different current distribution, those are also different from the antenna_1 and antenna_2.

Figure 4-3 Multi-antenna Layout

As mentioned above, the bandwidth of Sub-6G antenna system doesn't increase dramatically, to achieve the high data throughput of 5G requirement. More antennas are needed for Sub-6G devices to realize the MIMO capability. The major challenge of sub-6G antenna design is from the increasing of the antenna number and band number. And there are still other existing antennas in the sub-6G phones, such as LTE antennas, WiFi antennas, Bluetooth antennas, GNSS antennas. In addition, higher display to body ratio is still the trend of future phone design. They all give more threatening for antenna environment.

To meet the performance requirements, sub-6 GHz antenna should be carefully designed and optimized from pattern layout and architecture placement.

To get better MIMO performance, some studies have been done to get better isolation and correlation as shown in following graph

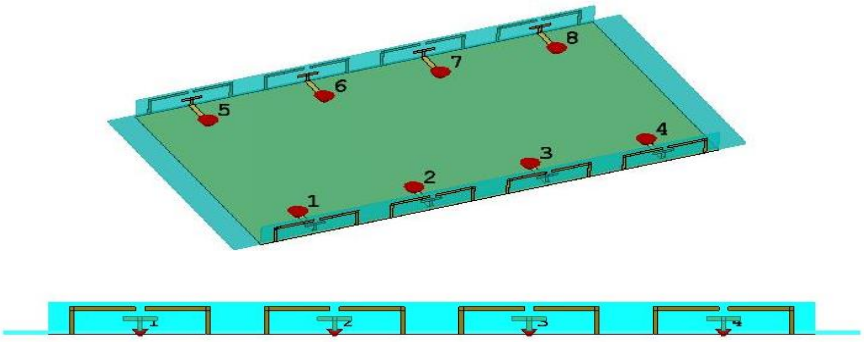

Figure 4-4 Self-Isolated Antenna Element

As is seen, an 8-element antenna model that operates at 3.3-3.8Ghz was studied. The single antenna element was special designed, that has self-isolation property, and Isolation element is also a part of the antenna (no additional isolation element is needed!). As a result, isolation is better than -21dB, and Antenna efficiency is better than 60%. So, MIMO antenna system can have good isolation & efficiency

In summary, the multi-antenna system applied to 5G devices, each antenna should have high efficiency and good independence. These two points can be measured respectively by efficiency and passive ECC (Envelope Correlation Coefficient). In smartphone design, TRP and TIS in SISO condition and active ECC between each SISO path should be required.

Passive performance like efficiency, VSWR (Voltage Standing Wave Ratio), isolation and are important metrics in antenna design.

Due to close frequency range, the way to test VSWR, isolation, efficiency/gain and ECC (envelope correlation coefficient) of Sub-6G antenna is the same with that of traditional LTE antenna.

For VSWR and isolation test, VNA with S-parameters is widely used. Since there are more antennas (8X8, 4X4, 4X2) in one device, more ports of VNA will make isolation test more convenient and efficient. Figure 4-5 shows typical test results of current Sub-6G antenna design.

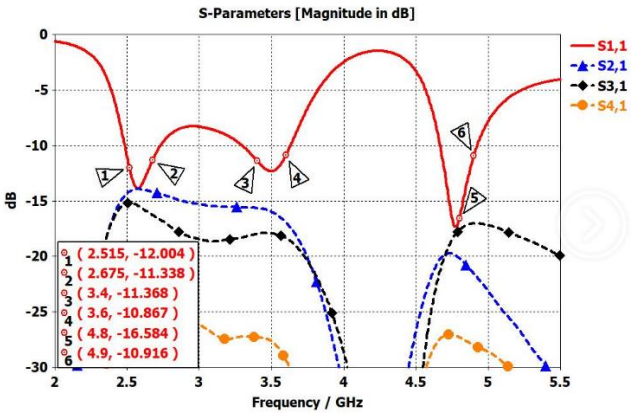

Figure 4-5 S-parameters of Sub-6GHz antenna

For efficiency/gain test, traditional anechoic chamber system (ETS-Lindgren, Satimo) can be also used for Sub-6G antenna. Figure 4-6 shows typical results of current design.

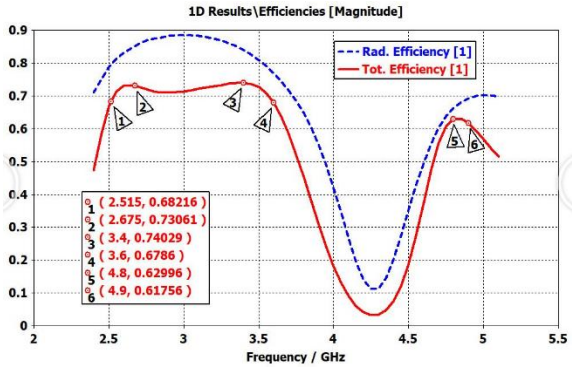

Figure 4-6 Efficiency of Sub-6GHz antenna

Since ECC (envelope correlation coefficient) takes into account the antennas' radiation pattern shape, polarization, and even the relative phase of the fields between the two antennas, anechoic chamber system (ETS-Lindgren, Satimo) can be also used to caculate the result of ECC.

Both ETS-Lindgren and Satimo system have the calculation function of ECC (envelope correlation coefficient) based on radiation pattern of antennas.

5 mmWave Device antenna

5.1 Introduction

Webster's Dictionary defines an antenna as "a usually metallic device (as a rod or wire) for radiating or receiving radio waves". The IEEE Standard Definitions of Terms for Antennas (IEEE Std 145 – 1983)* defines the antenna or aerial as "a means for radiating or receiving radio waves." In other words the antenna is the transitional structure between free-space and a guiding device. Some antenna definitions are listed and explained: ***(a) radiation pattern:*** An antenna radiation pattern or antenna pattern is defined as "a mathematical function or a graphical representation of the radiation properties of the antenna as a function of space coordinates; ***(b) radiation power density:*** The quantity used to describe the power associated with an electromagnetic wave; ***(c) radiation intensity:*** in a given direction defined as "the power radiated from an antenna per unit solid angle." The radiation intensity is a far-field parameter, and it can be obtained by simply multiplying the radiation density by the square of the distance; ***(d) beamwidth:*** The beamwidth of a pattern is defined as the angular separation between two identical points on opposite side of the pattern maximum; ***(e) directivity:*** defined as "the ratio of the radiation intensity in a given direction from the antenna to the radiation intensity averaged over all directions".

There are lots of antenna forms, which can be briefly classified into the following types: wire antennas, aperture antennas, microstrip antennas, array antennas, reflector antennas and lens antennas. Here some most common used device antennas are introduced:

Printed antennas, broadside radiation: produced by standard lithographic processes, where metal is printed on top of a substrate. The most common types of printed antennas are patches, dipoles and variations of these, as shown in Figure 5-1. The advantages of this type antenna can be elaborated: simplest form inexpensive to fabricate, low in profile and light in weight. Their size is in the order of the resonance wavelength, which make them array compatible to obtain higher gain values, but also opens up new interation options at mmWave frequencies. And the disadvantages are concluded: on chip printed antennas have both low radiation efficiency and negative gain.

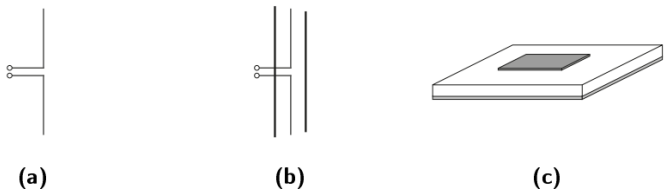

Figure 5-1 Different kinds of printed antenna types (a) a dipole antenna, (b) a yagi antenna, (c) a rectangular patch antenna.

Substrate Integrated Waveguide Antennas (SIW): SIW is a technique that can be employed to

construct integrated antennas. The general appearance of a SIW circuit are a dielectric layer between a top-and bottom metal clad while rows of metalized via holes act as side walls. An example with end-fire radiation is shown in Figure 5-2. SIWs can be realized through low-cost standard PCB processes making it possibly suitable for mass production. However, the use of SIW technology is not only restricted to antenna construction, but its advantages are more related to the possibility of integrating an antenna with other circuits on a single substrate. Thus, many encountered design proposals address an antenna together with a beamforming network.

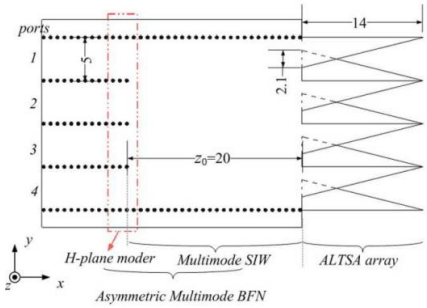

Figure 5-2 SIW multi-beam antenna with asymmetrical BFN on a single substrate

Magneto-Electric Dipole Antennas: an example of ME dipole can be seen in Figure 5-3, where the planar top metal layer acts as an electric dipole while the vertical pins act as a quarter-wavelength patch. The antenna achieved a very wide bandwidth, maximum gain of 7.5dBi and a radiation pattern similar to a regular patch antenna.

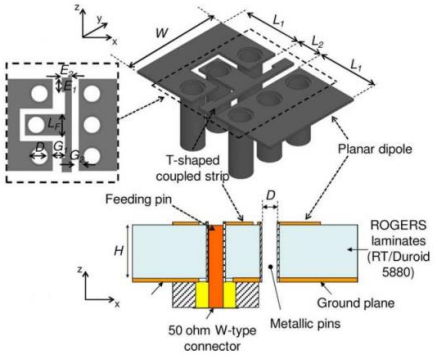

Figure 5-3 Electro-magnetic dipole antenna

Refer to millimeter antennas in device applications, the antennas need to be integrated with the RF circuit due to high interconnection loss, lead to new antenna forms of AoC and AiP developed.

Antenna on Chip (AoC) : integration of an antenna on the same chip as other circuits using standard technologies. The most common types of on chip antennas are printed antennas, since there are suitable for integration with solid-state devices, but a certain amount of dielectric resonators have also been encountered. A typical model of an antenna mounted on

a Si IC chip can be seen in Figure 5-4.

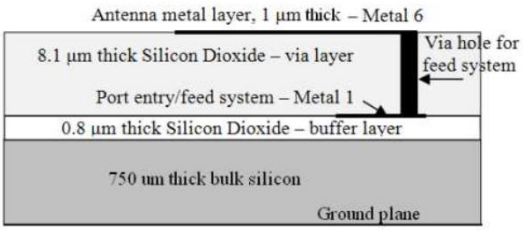

Figure 5-4 Cross sectional view of a typical IC model for antenna on chip simulation set up

Advantage: connections between the RF circuit and the radiating element, a significant cost reduction can be realized. By producing the antenna in the same process as the rest of the circuit, several manufacturing issues can be removed, while simultaneously suppressing losses that would otherwise occur in the complex interconnections.

The on chip antenna solution is still under development, and has not come far enough to enable performances meeting the requirements for commercial usage. It has both very low radiation efficiency and gain. The major concern regarding on chip antennas is the low radiation efficiency. Si substrates have a relatively low resistivity which causes ohmic losses in the substrate and hence reduce the radiation efficiency. These losses can be reduced by using selective ion- or proton implantation which increases the resistivity, however this directly indicates an increased cost. Moreover, losses also occur due to power trapped in surface waves. This does not only reduce the radiation efficiency, but also introduces mutual coupling. Due to the fact the circuit and the antenna are in close vicinity of one another, mutual coupling occurs between the different components one needs to understand the different coupling mechanisms. Suitable architecture and the use of ground shields have been shown to reduce the cross talk. Substrate thinning and the use of substrates with low dielectric constant, can help to reduce the power lost through surface waves.

Antenna in Package (AiP): antenna or array put in the same chip package as the radio frequency die. By using multilayer techniques, an antenna can be integrated in the package, which in turn offers more degrees of freedom regarding the design complexity. An example of an AiP solution is shown in Figure 5-5.

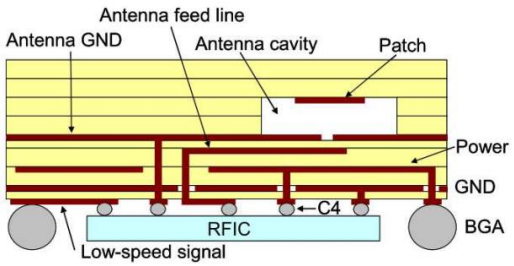

Figure 5-5 Cross sectional view of LTCC multilayer packaging with in package patch antenna

Different enhancement techniques can be implemented by controlling each layer, AiPs have shown good performances in terms of bandwidth and gain. Interconnection between the chip

and the package can then be established by either wire bonding or flip-chip bonding. By having the freedom to place the RF die almost arbitrarily, one can minimize the impact the active devices in the chip have on the antenna performance. The available volume and area for antenna implementation is not as restricted as for AoCs, which makes array configurations compatible. Also, compared to on chip antennas a broader variety of different antenna types have been presented for the in package solution, mainly due to the flexibility that applies to multilayer structures. Thus, the antenna types that have been encountered are more focused around the certain types that have shown good performance in the millimeter range and are not as restricted to outside factors. However, interconnections are usually made through wire bonding or flip-chip bonding, where wire bonding is the more commercially used. The wire-bonding technique is robust and inexpensive, but the long wires introduced act as inductors and affect the performance of the whole system. Apart from this, the main issues of in package antennas are more related to the actual package design.

Antenna on Structure (AoS): antenna design integrated with the UE device structure. With the benefit of the UE structure to design the radiators, lead to low cost and saving space. An example of an AoS solution is shown in Figure 5-6.

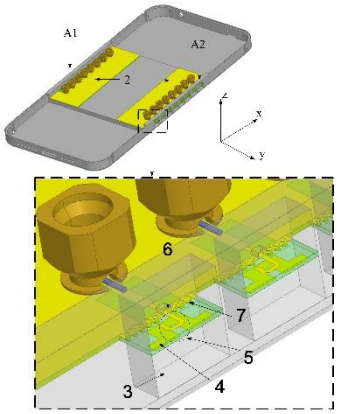

Figure 5-6 Cavity backed slot antenna array with AoS solution

The antenna-on-board (AoB) solution features the integration of antenna together with other front-end circuits on the same board. The location of the antenna module and the optimization of the radiation characteristic can be much more flexible. However if the antenna module is not near the RFIC, the interconnection between the antenna module and the RFIC might be difficult. Also, the interconnection loss will increase.

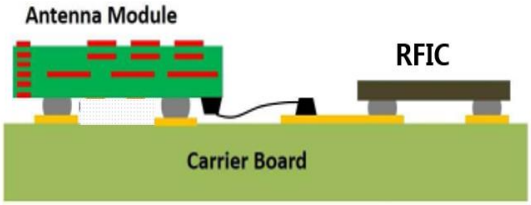

Figure 5-7 AoB solution illustration

In summary, the device millimeter wave antenna can be divided into two categories, one is

integrated with the chip, and the other is a distributed antenna. The first type of antenna has high integration and insertion loss, which is conducive to standardization. The second type of antenna is flexible in use, and can fully utilize the architecture design and structure space of the device to select an appropriate antenna position and implementation manner. The disadvantage is that the feed system is complex and the path loss is large.

For millimeter wave array antennas, choosing the right substrate is intuitively important for antenna performance. Materials that suitable for the device mmWave antennas include high-resistivity silicon, Teflon, ceramics, polymers and so on. Among them, low temperature cofired ceramic (LTCC) and liquid crystal polymer (LCP) materials and associated process technologies are particularly promising. LTCC technology has traditionally been preferred due to their superior dissipations. However, achieving accuracies acceptable for mmWave device applications at a low cost remains an issue for further improvement. LCP technology has been widely used for mmWave antennas in recent years due to its mechanical and design flexibility. Compared to LTCC technology, LCP has lower dielectric constant and slightly higher loss tangent. More importantly, LCP is capable of creating near-hermetic homogeneous multilayer dielectric laminations at a temperature of 285°, which is low enough to potentially package both active and passive devices into a compact module.

5.2 Design philosophy and principle

To compensate the high propagation loss of mmWave, beamforming arrays are needed in device. The beam direction can be controlled by the phase difference among the adjacent radiators. The beamforming technology is considered as an effective approach to mitigate the high path loss and attenuation loss in mmWave band. mmWave beamforming at the UE end is more difficult than at the BS end since it is largely constrained by high energy efficiency requirement, limitations in battery life and hardware dimension which are key FOM contributors. The use of array configurations of antennas makes it possible to not only increase the total gain by using many elements, but also radiate power in a desired angular direction (phased array system). An array configuration of identical element equal spacing introduces the array factor, from which the total far-field radiation of the array can be found from the radiation vector of the basic element.

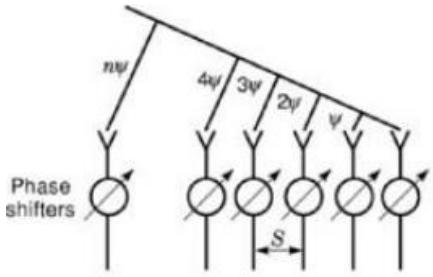

Figure 5-8 Block diagram of a phased array system

The development of a phased array consists of two major parts: the beam-forming network and the radiating element design. The element design is arguably the most critical part to

phased array antenna performance. To select a proper radiating element for the phased array antenna, a number of conditions must be known: the application, the volume constraints, and the environment in which the phased array antenna will operate.

There are also high-level design constraints between the wireless subsystem and device components. Besides the power budget and hardware area allocation, one more critical technical challenge originates from the interference among different components. For example, the display screen can cause the RF sensitivity degradation. Therefore, a sheet of metallic microwave (MW) shield is normally put between the display unit and hardware part to enhance the isolation. Moreover, this MW shield can minimize the SAR in the common use cases when the screen side is held close to the head of a smart phone user. In other words, antennas radiate minimal signal through the screen, and therefore it can only propagate the signal in the direction away from the human head. Nevertheless, the shield increases the thickness of the handset and degrades the form factor. The placements of camera, speaker, finger scanner, battery, MLB, also require careful consideration as they can change the electromagnetic (EM) field and lead to undesired effects. To summarize here, contemporary wireless UEs need to provide high quality of user experience determined and contributed by comprehensive factors which not only lie in the wireless system design, but also mechanical design, product design, operating system design, etc. Consequently, many design trade-offs must be considered for a high-performance 5G UE.

In the device design, the millimeter wave antenna also has the following design challenges:

1) Gain coverage

In order to maintain high data rate transmission with low latencies in mmW 5G mobile networks, it is essential to achieve high gain over a spherical coverage. However, planar phased-arrays inherently exhibit limited beam scanning coverage and this will likely result in wireless coverage blind spots. A practical solution is the combination the end-fire and broadside radiations with multiple antenna chips. An example is shown in Figure 5-9, where two antenna chip are located in the corner of the UE. Each antenna chip has one 2×2 patch array for broadside radiation and two 1×2 dipole arrays for end-fire radiation. It is worth pointing out that antenna with dual-polarization functions is appreciated when the wireless link budget attributed to polarization mismatch is considered.

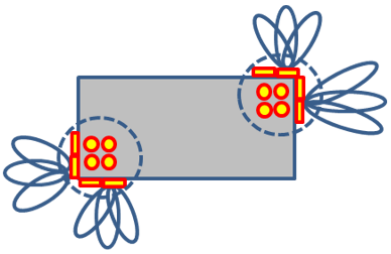

Figure 5-9 Block diagram of a phased array system

2) Antenna layout

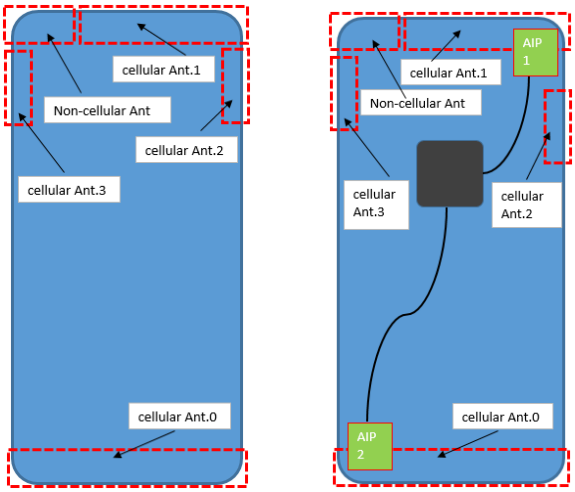

(a) (b)

Figure 5-10 (a) Typical layout. (b) Proposed layout.

Figure 5-10 (a) shows a typical antenna placements in a smartphone. Figure 5-10 (b) shows a proposed layout of the mmW 5G antenna for future cellphones. The-front end modules and RFICs are integrated with each of the phased-arrays for a low profile. Each mmW 5G antenna modules are connected to the baseband and digital chip through wired connections such as coaxial cables in the case of either direct-conversion or IF-architecture.

The layout of the millimeter wave antennas should also consider the interaction with the sub 6G antennas.

3）Antenna miniaturization

Millimeter wave antennas for devices need to consider small size requirements in addition to high gain and support for multiple frequency bands. Because the design of device products, especially mobile phones, is becoming more and more compact, large batteries and more functional components are almost full of the internal space of the mobile phone. Due to the pursuit of large screen ratio, the designers of the device hope that the millimeter wave antenna can be made smaller and smaller.

6 Evaluation for Sub-6G 5G Devices

6.1 Discussion on performance

6.1.1 Radiative OTA performance

6.1.1.1 Transmit power performance

The transmit power performance is normally related to the total radiated power (TRP). The TRP is given under a certain output power, e.g. maximum output power.

The maximum output power is important for UL performance. As shown in Figure 6-1, the coverage is evaluated for NR UE at 2.6GHz under different maximum output power levels for urban environment. It can be observed that up to 21% and 14% gain can be achieved for 26dBm vs. 23dBm and 25dBm vs. 23dBm respectively. And 1dB decrement from 26dBm maximum transmit power will lead to about 7% coverage degradation.

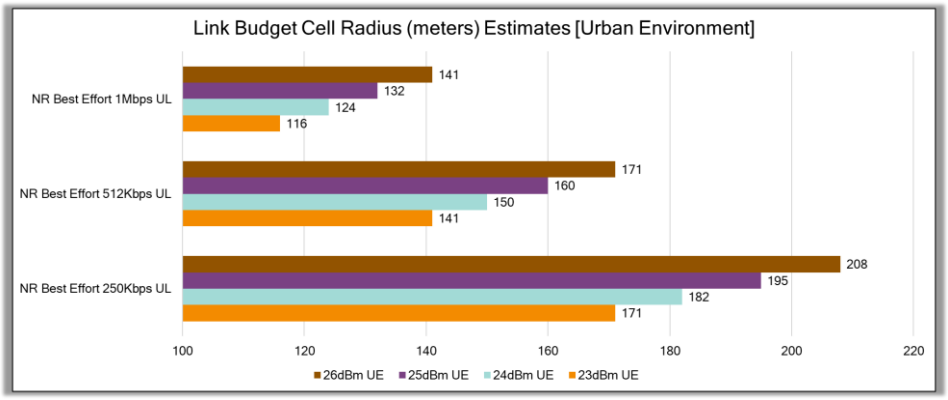

Figure 6-1 Coverage assessment with different maximum transmit power

Moreover, the evaluation for 80% outdoor + 20% indoor coverage and indoor only coverage are also presented in Figure 6-2 and Figure 6-3 respectively. It can be observed that up to 2.9% and 31% gain (26dBm vs. 23dBm) can be achieved for outdoor+indoor and indoor scenarios respectively.

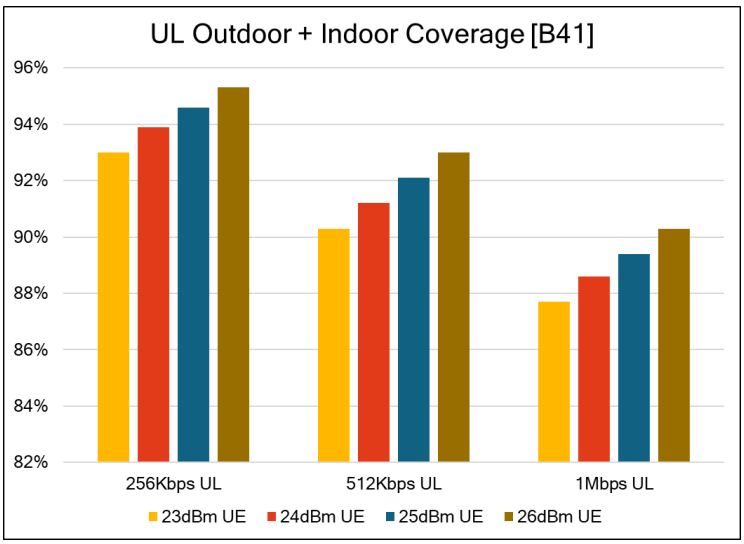

Figure 6-2 UL Outdoor + Indoor coverage performance

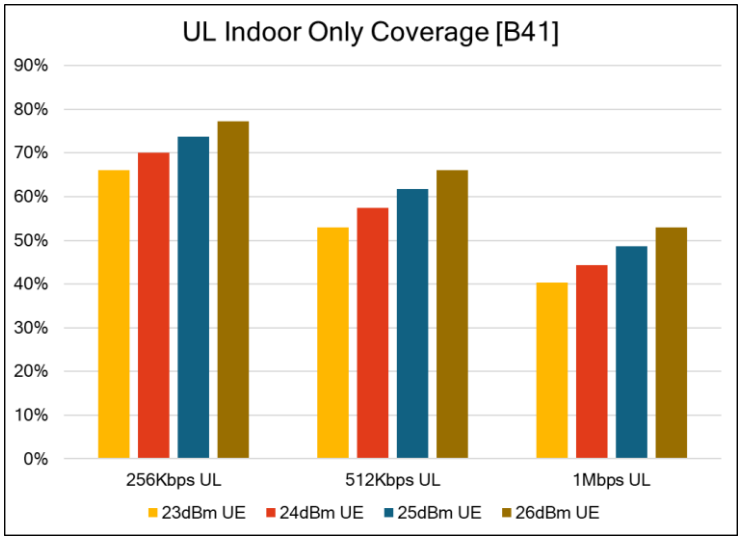

Figure 6-3 UL Indoor only coverage performance

From UE throughput's perspective, the evaluation on single user throughput is given in Figure 6-4, and 31% and 21% gain can be achieved for 26dBm vs. 23dBm and 25dBm vs. 23dBm respectively. Moreover, 1dB decrement from 26dBm maximum transmit power will lead to about 10% user throughput degradation.

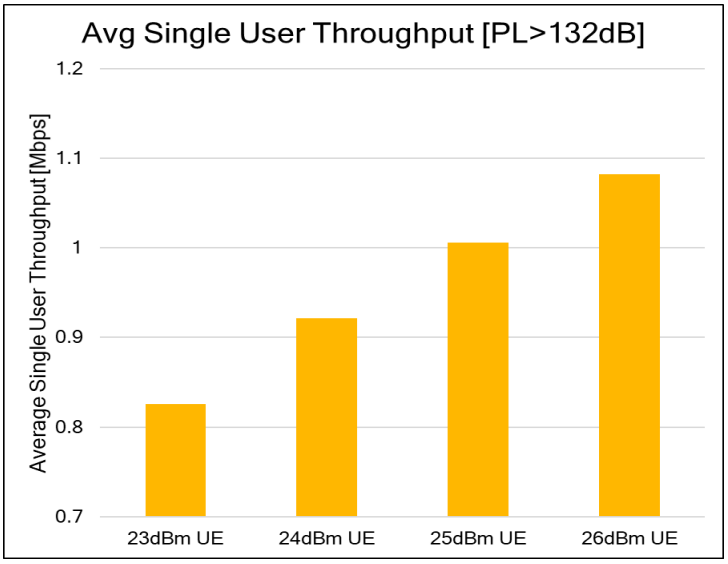

Figure 6-4 Average single user throughput with pathloss more than 132dB

It should be noted that TRP performance is very related with UE maximum transmit power. Therefore, TRP performance has a big impact on UL performance. With the increment of TRP, significant improvement on both UL coverage and user throughput can be achieved.

Comparing with the TRP measurement of the LTE devices, some new features occurs when evaluating the 5G NR devices. Mobile devices such as wireless handsets have used multiple (often two) omni-directional antennas for antenna diversity. For the previous telecommunication (e.g. 3G, 4G), the antenna diversity permits receiving signal only. However, for 5G NR UE, this technology is implemented for UL. Thus MIMO (multiple input, multiple output) transmission is allowed from the mobile to the base station. The idea here is multiple independent data streams to maximize throughput and as a result improve the performance of the transmit signal. So the TRP measurement of the transmit diversity (e.g. 2 TX for 5G NR UE) should be carefully discussed. As the wireless devices are operated in arbitrary positions. Furthermore, signal propagation will create signals arriving from arbitrary directions. As a result, full 3D evaluation is required to assess the impact on antenna performance of multipath reception, from all angles of arrival (AoA). A test approach that makes it possible to locate either of the two transmit test antennas at any point on a sphere centered on the DUT, providing simulated real-world test conditions.

There are two basic deployment policies for 5G network SA and NSA. For SA, the NR system can work independently with LTE. Thus a single connectivity with NR network is the basic operation for the UE. For NSA, UE may also encounter the in-device interference issue (such as LTE Band 4 and NR n 41) as the dual-connectivity of LTE and NR is supported in this case. However, it should be mentioned that this in-device interference could be identified during RF conductive test (e.g. EVM, ACLR, SEM, etc.)

So the TRP measurement could pay more attention to the final performance of the transmit power of the device.

6.1.1.2 Receive sensitivity performance

5G receiver sensitivity performance mainly means the UE sensitivity in OTA environment, i.e. TRS. The TRS has been widely used in 3G and 4G stage to evaluate UE antenna performance. In 5G era, however, it becomes more complex due to more receive antennas and LTE/NR interference in NSA.

For SA, 4Rx antenna is mandatory for n41, n77, n78 and n79. More antennas means more difficult in UE antenna design due to more cross coupling. From OTA performance evaluation perspective, there may be not much difference.

For NSA, besides more antennas in NR, the difference from SA is that LTE need to be working simultaneously. LTE and NR concurrent transmitting and receiving will lead to severe IMD or harmonics interference if the frequency choosing is not appropriate. However, these interference scenarios have already been considered in the RF conducted tests and no longer the key points in the OTA tests. What NSA TRS need to be considered is the antenna performance, in other words specific test frequencies should be chosen to avoid interference issue and test pure UE OTA performance is enough.

6.1.2 MIMO OTA performance

5G devices have 4 downlink antennas and 2 uplink antennas. By using techniques such as non-correlation in the propagation channel, MIMO can multiply the throughput of the communication system while not consuming additional spectrum and time domain resources. MIMO spatial multiplexing transform implementations support data rates almost twice as high as the data rates available from a single uplink antenna and fourth for single downlink. This higher data rate is possible through the use of spatial multiplexing, where the device's serving network simultaneously transmits two or four independent, spatially-diverse data streams to the wireless device.

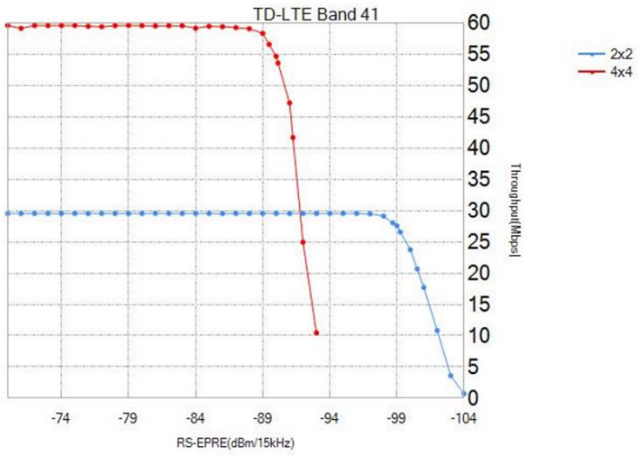

Figure 6-5 4x4 vs 2x2 MIMO OTA throughput performance

MIMO device can use information such as space domain, time domain, and frequency domain in the propagation environment to optimize the performance of the communication system based on the channel environment. Therefore, for the final MIMO device performance test and evaluation, the channel model is strongly dependent, that is, the channel model must be reproduced in the laboratory. Make MIMO device testing truly repeatable and controllable.

For 5G device, 4*4 downlink MIMO requires a larger design challenge for the balance between the four antennas, the matching circuit design, and the multi-band performance in a narrow space of the device. In order to realize the full benefit of spatial multiplexing, the wireless device must be able to differentiate between the uplink or downlink data streams. In order to assess radiated MIMO performance, the lab should establish a standardized spatial channel, with characteristics similar to real-world radio environments. Currently, the test system creates an SCME Urban Macro and Micro propagation channels as 2D channel models, and used the 3GPP 38901 3D channel models. However, any spatial channel model can be created within the test zone should future industry demands require the use of alternative models.

MIMO OTA mainly evaluate the average throughput performance of devices with multi antennas. Total Radiated Multi-antenna Sensitivity (TRMS) and the MIMO Average Radiated SIR Sensitivity (MARSS) are two most widely used metrics in MIMO OTA test. The above two metrics reflect devices' multi-antenna performance from different perspective.

In 3GPP, the MIMO OTA metric is Total Radiated Multi-antenna Sensitivity (TRMS) where the UE must meet or exceed data throughput levels defined as a percentage of the maximum throughput of the reference measurement channel (RMC). The cell power decreased step by step and no added noise in the test environment. With this method, the throughput is mainly sensitive to 3 metrics, namely, ECC, power imbalance and the antenna efficiency.

In CTIA, the metric used for MIMO OTA is MIMO Average Radiated SIR Sensitivity (MARSS) where SIR is the signal to interference ratio. With this method, the influence of power imbalance and antenna efficiency can be neglected due to the added noise is much higher than the noise floor device. The throughput performance is only sensitive to the antenna correlation.

MIMO OTA requires the minimum RS-EPRE/SINR at which the DUT can get 95% and 70% of the maximum throughput. Take the online video as an example, 95% throughput means the film is not so fluency and 70% represent the experience is not acceptable. Follow shows the test results under each methods.

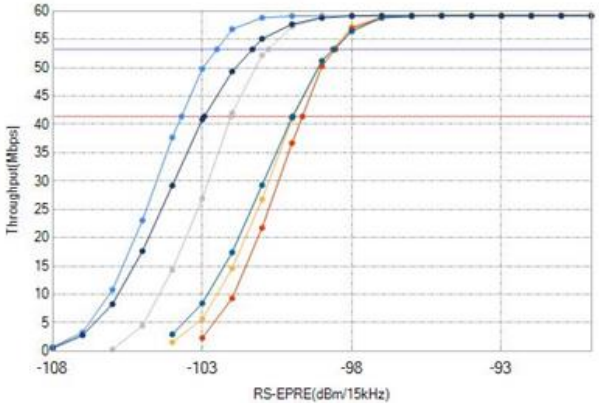

Figure 6-6 Comparisons of 6 different devices

6.1.3 MIMO antenna performance metrics

DUT's active antenna pattern contains all the antenna information, for example Figures 6-7, 6-8 and 6-9 show the gain of the first antenna, the second antenna and the relative phase between these two antennas for one 2D cut. Although interesting in themselves, Figures 6-7, 6-8 and 6-9 don't immediately reveal DUT MIMO performance directly [20]. This is typical of antenna-only metrics such as gain, branch power imbalance, phase, envelope correlation coefficient (ECC) etc. However, it is only when the device antenna pattern is convolved with the spatial channel model under test including the Tx antenna assumptions that it is possible to see the actual signal that will be presented to the receiver for demodulation.

Given the information of Tx antenna pattern, channel model and the Rx antenna pattern, it is possible to compute a wide variety of signal characteristics that can help predict and explain the variation in DUT performance. Equation (25) in [21] shows how to calculate the co-variance matrix for a general 3D scattering environment. With the MIMO channel co-variance matrix, MIMO antenna gains, power imbalance and correlation can be derived straightforwardly. With these statistical characteristics MIMO channel capacity also can be calculated with the assumption of SNR. Figures 6-10, 6-11 and 6-12 show the MIMO antenna gains, power imbalance and correlation vs rotation angle under UMi channel model. In Figure 14 the curve denoted by (2, 1) represents the correlation for receiver side, that denoted by (3, 1) represents the correlation for transmitter side.

For the spatial directional channel model such as Umi, the signal angular distribution is not uniform in the space, the experienced signal characteristics by DUT are also variation as rotating DUT to different rotation angles. That's why Figure 6-10, 6-11, 6-12 and 6-13 show the properties and performance vs azimuth angle. It should be noted these three metrics are calculated based on the assumption of Tx, Rx antenna pattern and channel model info.

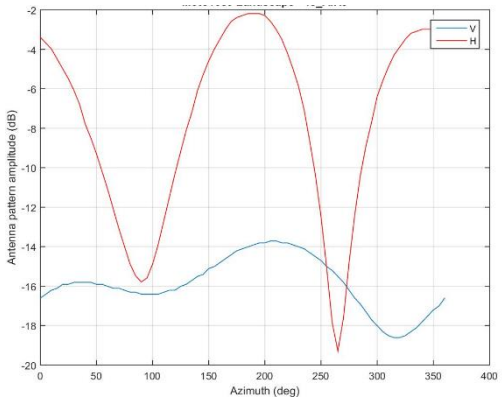

Figure 6-7 DUT gain for antenna 0 by azimuth

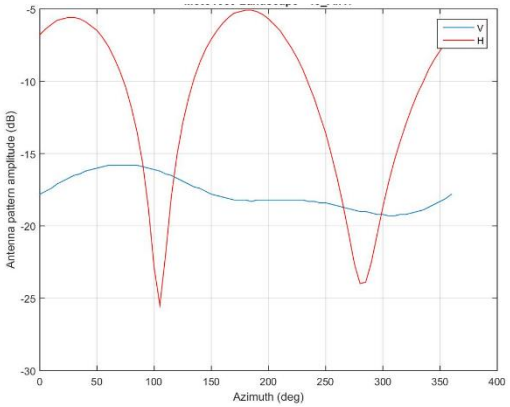

Figure 6-8 DUT gain for antenna 1 by azimuth

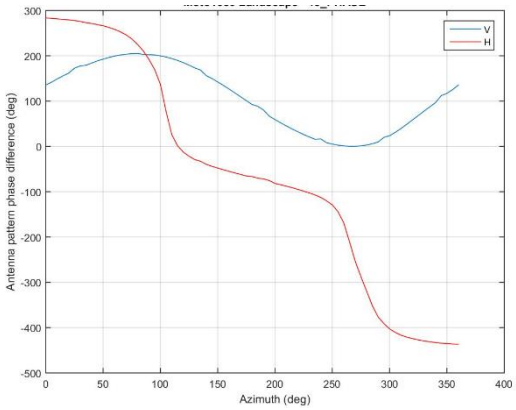

Figure 6-9 DUT relative phase between antenna 0 and antenna 1 by azimuth

It can clearly be seen that because the correlation and power imbalance keep in moderate level, which will not significantly impact the throughput performance, the shape and sense of the Figure 6-10 MIMO antenna gain closely matches the throughput curve variation in Figure

6-13. It can clearly be seen from Figures 6-10, 6-11 and 6-12 that there is a strong relationship between these two elements of the covariance matric and the observed variation in DUT throughput by azimuth. More relationship analysis can be found in [22]. Such insight into performance cannot be gained by direct analysis of the DUT antenna patterns alone. By analysis of these signal metrics the device and antenna designers can gain significant insight into optimizing performance based on spatial channel models.

Although the example used in this section is measured antenna pattern for DUT with two Rx antennas, for the uplink transmission when multiple antennas are equipped for Tx side the metrics in this section are also applicable for uplink MIMO antenna performance evaluation.

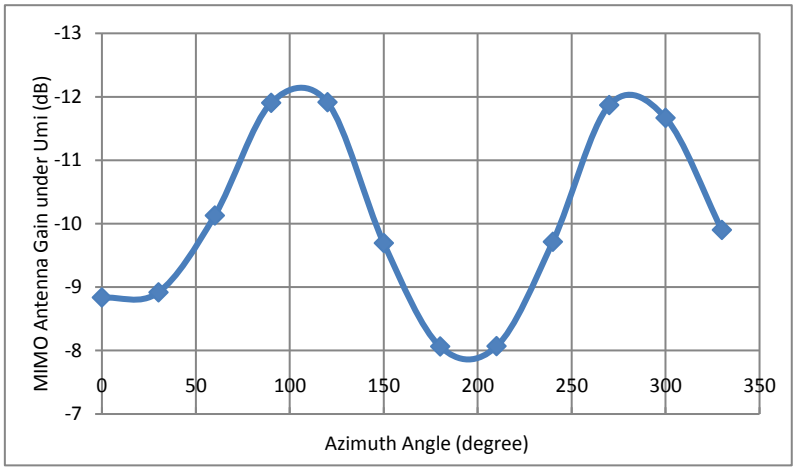

Figure 6-10 MIMO antenna gain by azimuth under Umi

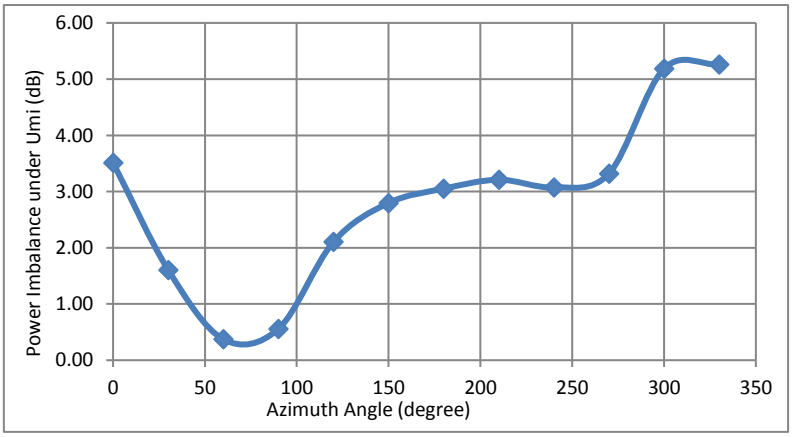

Figure 6-11 Received power imbalance between DUT two RF ports by azimuth under Umi

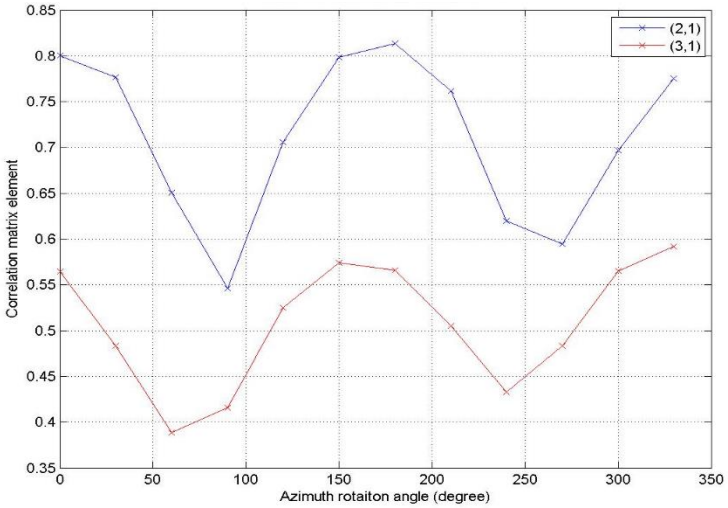

Figure 6-12 Rx and Tx correlation by azimuth under Umi

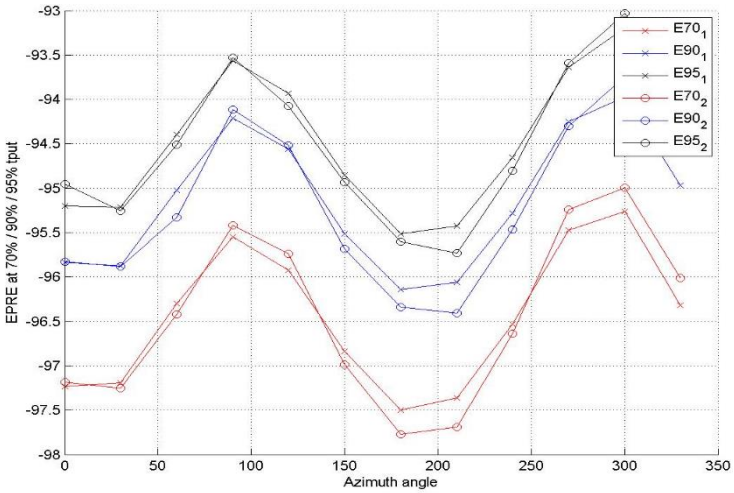

Figure 6-13 MIMO OTA performance by azimuth under Umi

6.2 Available Test methods

6.2.1 Single-Probe Anechoic Chamber (SPAC)

Two acceptable methods of scanning the EUT are proposed. The “great circle” cut method, whereby the Measurement Antenna remains fixed and the EUT is rotated about two axes in sequential order. The “conical” cut method, whereby the EUT rotates on its long axis and the measurement antenna is moved to several locations both above and below the level of the EUT for each rotation.

Figure 6-14 below shows the typical setup using a combined-axes system (the great circle cut

method). In addition to the pictured theta-axis rotation, the EUT will have to be rotated about the Z-axis (phi rotation) in order to perform the full spherical scans.

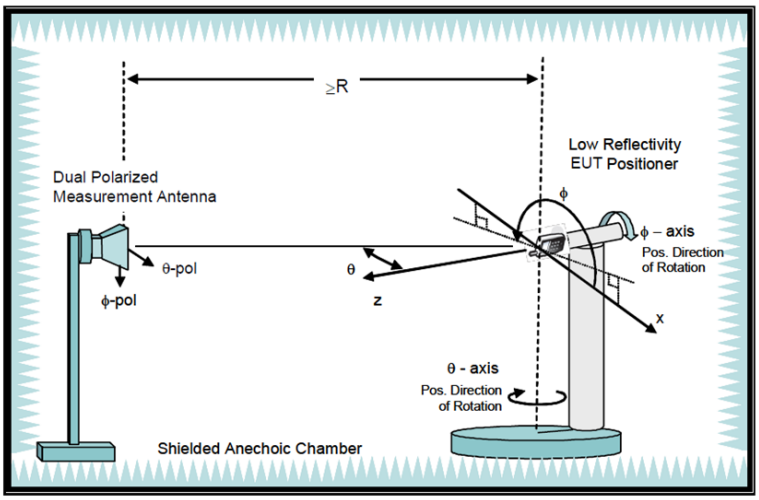

Figure 6-14 Typical setup for a combined-axes system

Figure 6-15 below shows the typical setup using the distributed-axes system (the conical cut method). In this configuration, the phi and theta angles are traversed separately by the distributed positioners in the chamber.

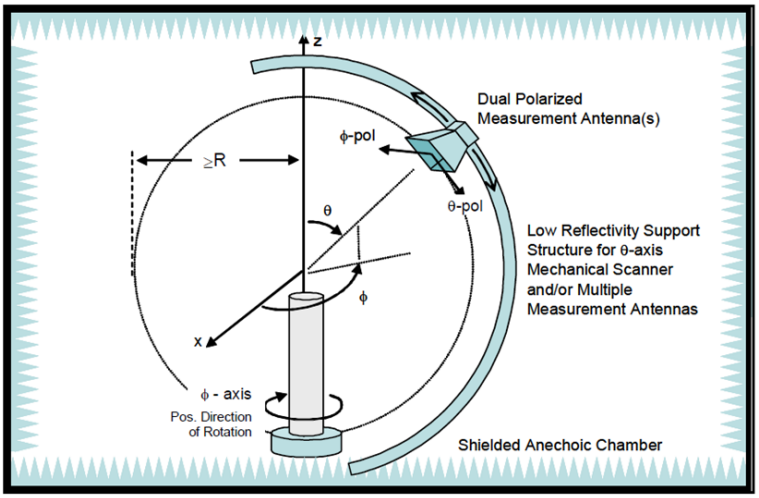

Figure 6-15 Typical setup for a distributed-axes system

6.2.2 Multi-Probe Anechoic Chamber (MPAC)

6.2.2.1 General introduction

The Multi-Probe Anechoic Chamber (MPAC) is based on the anechoic boundary array concept.

The anechoic boundary array refers to a mechanism by which any desired near-field RF environment can be created, subject to the limitations imposed by the resolution of the boundary array and the channel emulation applied. By arranging an array of antennas around the Device Under Test (DUT), a spatial distribution of angles of arrival may be simulated to expose the DUT to a near field environment that appears to have originated from a complex multipath far field environment. The anechoic chamber only serves to isolate the test volume from the external laboratory environment and to minimize unwanted internal reflections in the region of the DUT. It is assumed to play no part in the environment generated.

Spatial channel model with appropriate channel impairments such as Doppler and fading are applied to each path prior to injecting all of the directional signals into the chamber simultaneously through the boundary array. The resulting field distribution in the test volume is then integrated by the DUT antennas and processed by the receivers just as it does in real world multipath environment.

Follow shows the structure of MPAC which can be used for both UL and DL MIMO OTA test. The multi-cluster spatial channel models used to evaluate the DUT, a boundary array distributed as an azimuthal ring about the DUT is considered sufficient to adequately reproduce the target channel models. The transmit link should be established separately for the UL and DL MIMO test, such as the circulators and PAs which should be used to have a sufficiently large dynamic range for downlink and uplink signals.

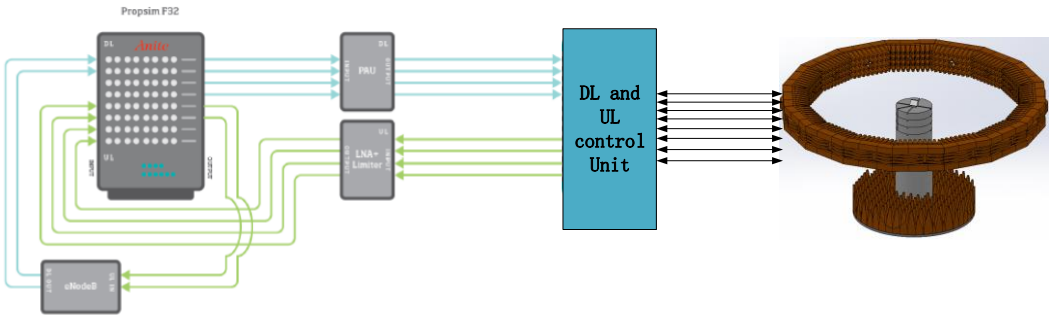

Figure 6-16 System configuration

6.2.2.2 Channel Model Definition

The most widely used channel model is the Spatial Channel Model extension (SCME) model which consist of two scenarios, the Uma (Urban macro-cell) and Umi (Urban micro-cell). The configuration are shown in table 6-1 and table 6-2 separately.

Table 6-1 SCME Urban macro-cell

SCME Urban macro-cell								
Cluster #	**Delay [ns]**			**Power [dB]**			**AoD [°]**	**AoA [°]**
1	0	5	10	-3	-5.2	-7	82.0	65.7
2	360	365	370	-5.2	-7.4	-9.2	80.5	45.6
3	255	260	265	-4.7	-6.9	-8.7	79.6	143.2
4	1040	1045	1050	-8.2	-10.4	-12.2	98.6	32.5
5	2730	2735	2740	-12.1	-14.3	-16.1	102.1	-91.1
6	4600	4605	4610	-15.5	-17.7	-19.5	107.1	-19.2
Delay spread [ns]								839.5
Cluster AS AoD / AS AoA [°]								2/35
Cluster PAS shape								Laplacian
Total AS AoD / AS AoA [°]								7.9/62.4
Mobile speed [km/h] / Direction of travel [°]								30/120
XPR *NOTE*: V & H components based on assumed BS antennas								9 dB
Mid-paths Share Cluster parameter values for:								AoD, AoA, AS, XPR

Table 6-2 SCME Urban micro-cell

SCME Urban micro-cell								
Cluster #	**Delay [ns]**			**Power [dB]**			**AoD [°]**	**AoA [°]**
1	0	5	10	-3.0	-5.2	-7.0	6.6	0.7
2	285	290	295	-4.3	-6.5	-8.3	14.1	-13.2
3	205	210	215	-5.7	-7.9	-9.7	50.8	146.1
4	660	665	670	-7.3	-9.5	-11.3	38.4	-30.5
5	805	810	815	-9.0	-11.2	-13.0	6.7	-11.4
6	925	930	935	-11.4	-13.6	-15.4	40.3	-1.1
Delay spread [ns]								294
Cluster AS AoD / AS AoA [°]								5/35
Cluster PAS shape								Laplacian
Total AS AoD / AS AoA [°]								18.2/67.8
Mobile speed [km/h] / Direction of travel [°]								30/120
XPR *NOTE:* V & H components based on assumed BS antennas								9 dB
Mid-paths Share Cluster parameter values for:								AoD, AoA, AS, XPR

6.2.2.3 Base Station Antenna Pattern

The emulated base station antennas shall be assumed to be dual polarized equal power elements with a fixed 0λ separation, 45 degrees slanted.

The slant 45 degree antenna is an “X” configuration and is modeled as an ideal dipole with isotropic gain and subject to a foreshortening of the slanted radiating element, which is observed to vary as a function of the path angle of departure. This foreshortening with AoD represents typical slanted dipole behavior and is a source of power variation in the channel model. The effective antenna pattern for this antenna is illustrated in the figure below.

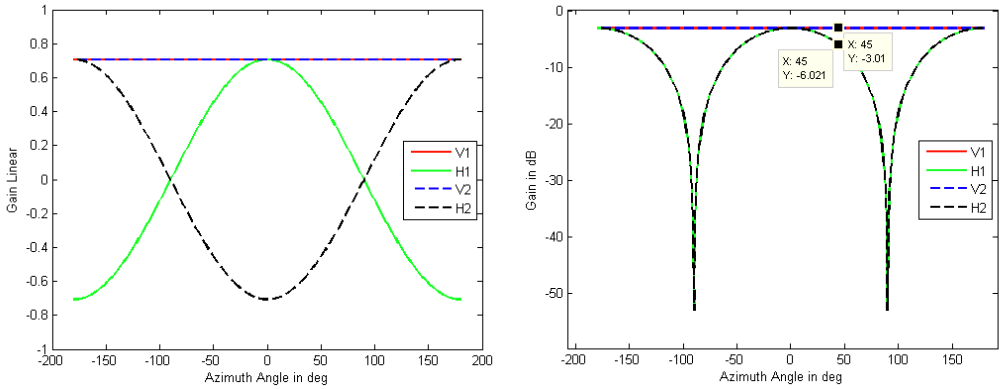

Figure 6-17 “X” ANTENNA GAIN ASSUMPTION (A) LINEAR GAIN (B) DB

To test 4x4 MIMO, it is proposed that the emulated BS antenna adds another set of dual polarized equal power elements with a fixed 0λ separation, 45 degrees slanted at a 0.50λ separation from the first. The total configuration is an “X X”.

Figure 6-18 2D planar array with cross-polarized elements 0.5λ separated

6.2.2.4 Test result averaging method

When performing MIMO performance test, DUT needs to rotate in the horizontal plane and conduct throughput test in different directions to obtain N throughput curve. After the test, the linear average method was first used to average the throughput curve of N bars under the same test attitude, and then the results of the throughput curve under different test postures were averaged, and the corresponding value of the target throughput was finally obtained.

$$P = 10\log_{10}\left[\sum_{n-1}^{N} 10^{\frac{P}{10}} / N\right] \quad (6\text{-}1)$$

6.2.3 Radiated Two-Stage (RTS)

6.2.3.1 General introduction

The RTS method utilizes a traditional SISO anechoic chamber but divides the MIMO OTA test into two stages: 1) In the first stage the device antenna pattern is measured. 2) In the second stage a channel emulator is used to convolve the measured antenna pattern with the desired channel model to provide the stimulus radiated throughput test on the DUT. To accurately measure the antenna patterns of the device, it is necessary for the DUT to support amplitude and relative phase measurements of the antennas. In the RTS method multipath fading, the

angular spread for transmit and receive sides and the XPR are all generated in the channel emulator enabling a simple anechoic chamber to emulate arbitrarily complex 2D or 3D channels. The test setup is shown in below figure.

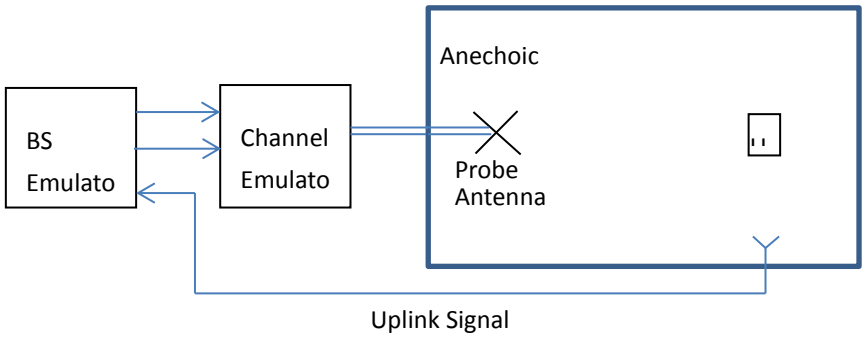

Figure 6-19 RTS MIMO OTA Test Setup

- **First stage: Antenna Pattern Measurement**

The first stage of RTS MIMO OTA test method is to acquire the DUT's antenna pattern. The non-intrusive antenna measurement approach uses the ability of the receiver in the DUT to measure the amplitude and relative phase of known signals incident at the DUT antennas. This capability is implemented as part of a test mode in the device. By rotating the DUT relative to the known incident signal it is possible from the DUT amplitude measurements and relative phase measurements between the antennas to construct the 3D antenna patterns and phase responses. To fully characterize the antennas, measurements are made at two orthogonal probe antenna orientations, typically vertical and horizontal. This can be done by switching between two separate antennas or by rotating a single antenna. DUT transmit the measured antenna pattern results to BS emulator over the uplink air interface which is active during the pattern measurements. This may take the form of an IP data connection with associated client application or using layer 3 signaling as defined in 3GPP TR 36.978.

- **Second stage: Throughput Measurement**

In the second stage, the desired antenna pattern is loaded into a channel emulator and convolved with the spatial channel model being used to evaluate the DUT performance. This process generates the signals at the DUT receiver that would have been received by the DUT been placed in the same 2D or 3D spatial field. The Advantage of this two-stage approach is that radio conditions representing arbitrarily complex 2D or 3D spatial channels can be emulated using a simple anechoic chamber with just two probe antennas for 2×2 MIMO test. During the second stage it is not necessary (or meaningful) to alter the device orientation relative to the probe antennas since the rotation of the DUT relative to the chosen channel model is performed electrically (and hence without error) within the channel emulator. The fully radiated Two-stage method setup is shown in Figure 6-9. This approach does require the use of an anechoic chamber for throughput measurements but has the benefit that any radiated interference generated by the device is fully taken into account in the measurements.

The purpose of the radiated connection is to enable the signals generated by the channel emulator, which are already conditioned to include the effect of the device antennas, to be directly connected to the device receiver. However, this can only be done by calibrating out the impact of the signal propagation in the anechoic chamber and the impact of the device antenna.

To achieve this calibration, it is necessary to measure the propagation conditions inside the anechoic chamber and modify the transmitted signals in such a way that the received signals look like the original unmodified signals. The process to achieve this is very similar to the precoding used to optimize signal reception for spatial multiplexing (MIMO) gain. Without signal conditioning, the first spatial stream S1 transmitted from probe antenna 1 will be received by both DUT antennas causing S1 to appear at different amplitudes and phases at both DUT receivers. Similarly, the second stream S2 transmitted from probe antenna 2 will also be received by both receivers at different amplitudes and phases. To create the desired situation where S1 is received only by receiver 1 and S2 is received only by receiver 2 it is necessary to calculate the transmission properties of the anechoic chamber then compute the inverse transmission matrix and multiply this by the two streams. The result is that both probes transmit copies of both S1 and S2 at different amplitudes and phases such that S1 is received only at receiver 1 and S2 is received only at receiver 2. This precoding process is not exact so the ideal, and the situation of complete isolation between the signals and receivers is not possible; however, measurements have shown that above 15dB isolation is achievable for most devices, and this is sufficient isolation not to impact the throughput test results. The isolation that can be achieved is optimized by using orthogonal polarizations used for the probe antennas and selected DUT orientation in the second stage test. The choice of DUT orientation for the radiated second stage is not critical but is chosen from the measured antenna pattern to avoid any nulls in either antenna which would otherwise reduce the achievable isolation.

RTS has the capability to emulate arbitrary 2D/3D fading channel models and can provide comparable throughput as MPAC. It is very cost-effective because it can reuse SISO chamber. What's more, this method can provide more enhanced diagnostic information (antenna pattern, ECC, antenna gain and gain imbalance), which is very helpful for R&D team to figure out the problems. The only limitation of this method is that the DUT needs to support delivery of antenna gain/phase.

Nowadays, RTS is formally approved by 3GPP as harmonized method with MPAC in 37.144 and 37.544, and it is CTIA v1.1 candidate test method for TM2 (transmit diversity) and TM3 (spatial multiplexing) mode.

6.2.4 Reverberation Chamber (RC)

6.2.4.1 Reverberation chamber channels

In a well-designed RC there are very many modes excited at the frequency of operation.

Almost every mode can be factorized into 8 plane waves. During a stirring sequence, the

modes change, thus the plane waves change amplitude and direction. If the RC operates well, over a stirring sequence incident the DUT will have experiences plane waves from an even distribution of angles on the sphere. This is illustrated in figure

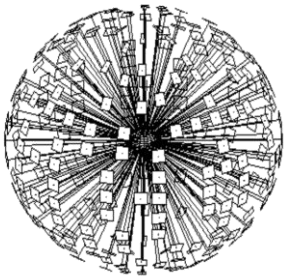

Figure 6-20 Plane wave distribution in an RC over a stirring sequence

Receives amplitude on an antenna port in an RC is Rayleigh faded over frequency and time (on the time scale of the stirring) and in space. This is illustrated in figure

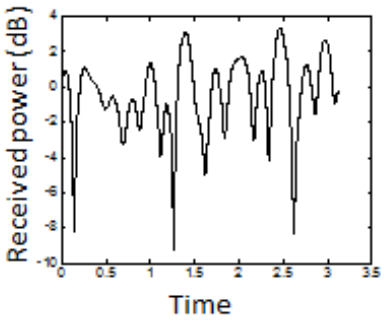

Figure 6-21 Rayleigh faded signal in reverberation chamber

Polarization balance is another important parameter in the RC. In a properly designed RC, there is polarization balance over a stirring sequence, with a distribution for different stirrer positions. This is illustrated in figure

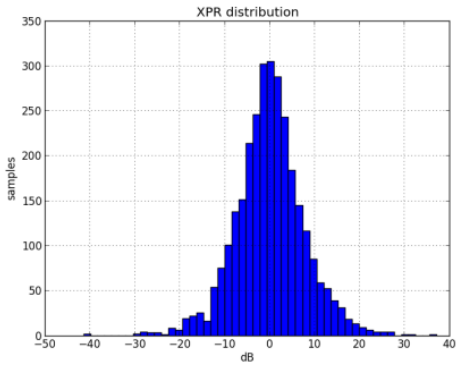

Figure 6-22 Polarization distribution inside reverberation chamber

Correlation between the fixed antennas in the RC can be controlled by design. The correlation

should be set to as low a value as possible to be able to test low correlated antennas (DUTs). In a well-designed RC, there should be a very low correlation between the fixed antennas in the RC.

6.2.4.2 Positioning and mode stirring facilities

The reverberation chamber shall be equipped with mode-stirring facilities in such a way that enough number of independent power samples can be achieved for the accuracy requirement stated in this standard to be fulfilled. Possible mode-stirring methods include platform stirring, polarization stirring and mechanical stirring with fan-type stirrers, irregular shaped rotational stirrers, or plate-type stirrers. Also frequency stirring is possible if the type of measurement allows for a frequency-averaged value, but this is not necessary if the chamber is sufficiently large and well stirred.

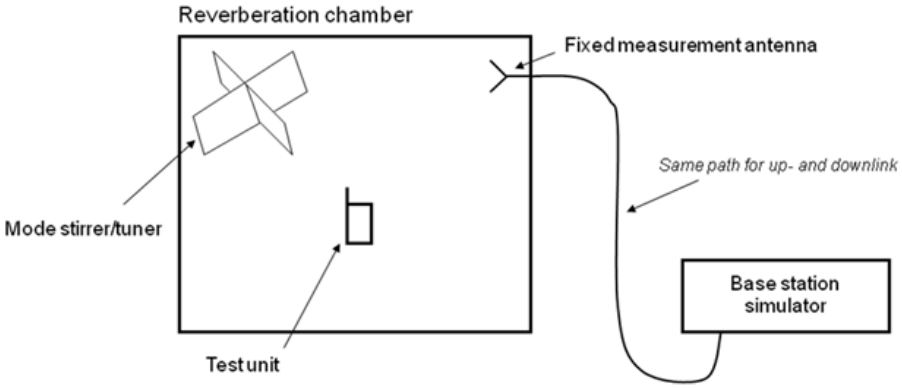

Figure 6-23 Reverberation chamber measurement setup

6.2.4.3 Measurement Antennas

It is important that the measurement antennas are configured in such a way that the statistical distribution of waves in the chamber in average corresponds to an isotropic environment.

6.2.4.4 Chamber size and DUT positioning

The reverberation chamber shall have a volume large enough to support the number of modes needed for the stated accuracy at the lowest operating frequency. If the UE/MS is moved around in the chamber during the measurement, the volume of the reverberation chamber can be reduced. Also, frequency stirring can be used to improve the accuracy, however, this will reduce the resolution of the results correspondingly.

The reverberation chamber can be loaded with lossy objects in order to control the power delay profile in the chamber to some extent. However the reverberation chamber should not be loaded to such an extent that the mode statistics in the chamber are destroyed. It is important to keep the same amount of lossy objects in the chamber during calibration measurement and test measurement, in order not to change the average power transfer function between these two cases. Examples of lossy object are head and hand phantoms.

Furthermore, the DUT must not be closer than 0.5 wavelengths to other electromagnetic reflective objects inside the chamber and 0.7 wavelengths to absorbing objects.

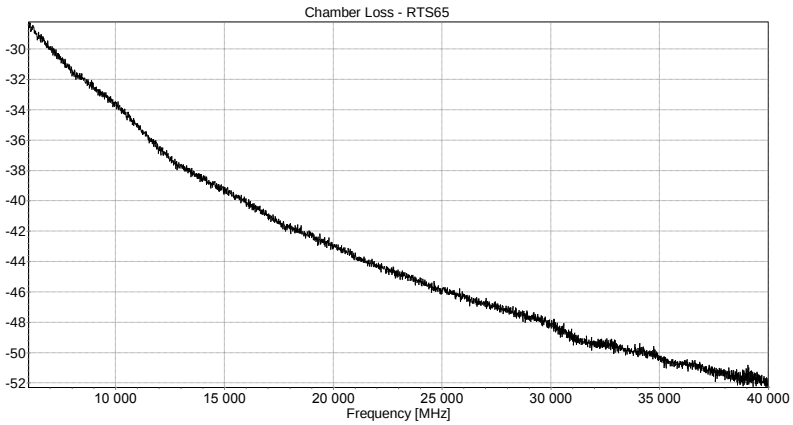

Figure 6-24 Chamber loss

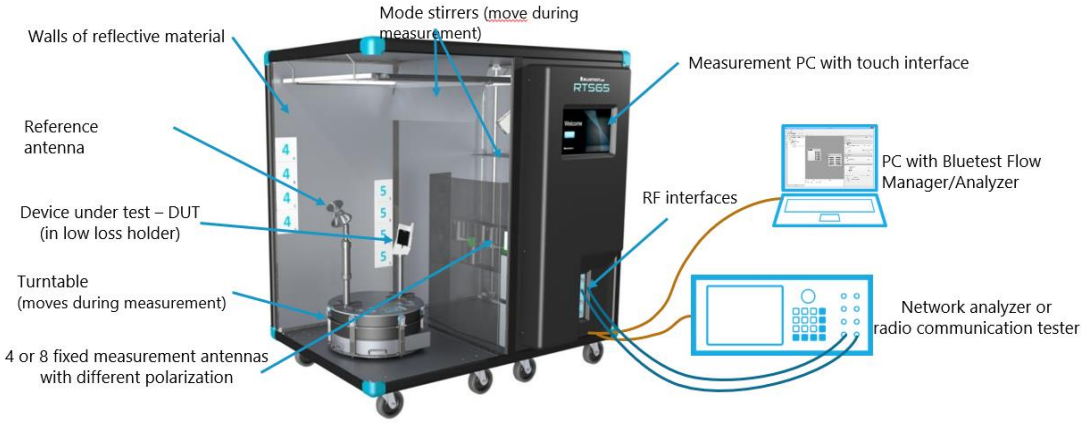

Figure 6-25 Measurement setup for MIMO TPUT measurements, utilizing a standalone reverberation chamber.

The following list of equipment is required to perform MIMO TPUT measurements.

- Reverberation chamber
- Radio communication tester
- RF cables (2 cables connecting the radio communication tester to the reverberation test system)
- Absorbers
- Applicable DUT holder
- Applicable phantoms (e.g. SAM head phantom, hand phantom or laptop phantom)

6.2.4.5 Measurement Metrics

- **TRP**

Definition and applicability

The Total Radiated Power (TRP) is a measure of how much power the DUT actually radiates. The TRP is defined as the integral of the power transmitted in different directions over the entire radiation sphere:

$$TRP = \frac{1}{4\pi}\oint\left(EIRP_{\theta}(\Omega; f) + EIRP_{\varphi}(\Omega; f)\right)d\Omega \tag{6-2}$$

Where Ω is the solid angle describing the direction, f is frequency. θ and φ are the orthogonal polarizations. $EIRP_{\theta}$ and $EIRP_{\varphi}$ are the actually transmitted power-levels in corresponding polarizations. Thus

$$TRP \approx \frac{\pi}{2NM}\sum_{n=0}^{N-1}\sum_{m=0}^{M-1}\left[EIRP_{\theta}(\theta_n, \phi_m; f) + EIRP_{\phi}(\theta_n, \phi_m; f)\right]\sin(\theta_n) \tag{6-3}$$

In these formulas N and M are the number of sampling intervals for theta and phi. θ_n and φ_m are the measurement angles.

The TRP can also be calculated from Rayleigh faded samples of the total power transmitted from the UE/MS. The measurement of transmitter performance in an isotropic Rayleigh fading environment is based on sampling the radiated power of the UE/MS for a discrete number of field combinations in the chamber. The average value of these statistically distributed samples is proportional to the TRP and by calibrating the average power transfer function, an absolute value of the TRP can be obtained. Thus

$$TRP \approx \frac{\sum_{n=1}^{N}\left(\frac{P_n}{C_n\left(1-R_n\right)}\right)}{\sum_{n=1}^{N}P_{ref,n}} \tag{6-4}$$

where $P_{ref,n}$ is the reference power transfer function for fixed measurement antenna n, R_n is the reflection coefficient for fixed measurement antenna n and C_n is the path loss in the cables connecting the measurement receiver to fixed measurement antenna n. These parameters are calculated from the calibration measurements. P_n is the average power measured by fixed measurement antenna n and can be calculated using the following expression:

$$P_n = \frac{\sum_{m=1}^{M}\left|S_{21,n,m}\right|^2}{M} \tag{6-5}$$

where $S_{21,n,m}$ is sample number m of the complex transfer function measured with fixed measurement antenna n and M is the total number of samples measured for each fixed measurement antenna.

Note that all averaging must be performed using linear power values (e.g. measurements in Watts).

- **TRS:**

Definition and applicability

The Total Radiated Sensitivity (TRS) is a measure of the minimum power required to achieve a specified Bit Error Rate (BER). The TRS is defined as:

$$TRS = \frac{4\pi}{\oint \left[\frac{1}{EIS_{\theta}(\Omega; f)} + \frac{1}{EIS_{\phi}(\Omega; f)} \right] d\Omega} \tag{6-6}$$

Where the effective isotropic sensitivity (EIS) is defined as the power available at the antenna output such as the sensitivity threshold is achieved for each polarization. Ω is the solid angle describing the direction, f is frequency. θ and ϕ are the orthogonal polarizations.

$$TRS \approx \frac{2NM}{\pi \sum_{n=0}^{N-1} \sum_{m=0}^{M-1} \left[\frac{1}{EIS_{\theta}(\theta_n, \phi_m; f)} + \frac{1}{EIS_{\phi}(\theta_n, \phi_m; f)} \right] \sin(\theta_n)} \tag{6-7}$$

In these formulas N and M are the number of sampling intervals for theta and phi. θ_n and φ_m are the measurement angles.

The TRS can also be calculated from measurements in a Rayleigh fading 3 dimensional isotropic environment with in average uniform elevation and azimuth distribution. The calculation of the TRS is in this case based on searching for the lowest power received by the LME for a discrete number of field combinations in the chamber that gives a BER that is better than the specified target BER level. By calibrating the average power transfer function, an absolute value of the TRS can be obtained. The following expression can be used to find the TRS:

$$TRS \approx 2N \frac{\left(\sum_{n=1}^{N} \left(C_n (1 - R_n) P_{thres,n} \right) \right)^{-1}}{\sum_{n=1}^{N} P_{ref,n}}. \tag{6-8}$$

where $P_{ref,n}$ is the reference power transfer function for fixed measurement antenna n, R_n is the reflection coefficient for fixed measurement antenna n and C_n is the path loss in the cables connecting the measurement receiver to fixed measurement antenna n. These

parameters are calculated from the calibration measurement and are further discussed in Annex B.2. $P_{thres,n}$ is calculated by using the following equation:

$$P_{thres,n} = \frac{\sum_{m=1}^{M} \frac{1}{\left|S_{21,n,m}^{thres}\right|^2}}{M} \quad (6\text{-}9)$$

where $S_{21,n,m}^{thres}$ is the m:th value of the transfer function for fixed measurement antenna n, which gives the BER threshold. M is the total number of values of the BER threshold power measured for each fixed measurement antenna.

MIMO TPUT:

Definition of MIMO throughput

MIMO throughput is defined here as the time-averaged number of correctly received transport blocks in a communication system running an application, where a Transport Block is defined in the reference measurement channel. From OTA perspective, this is also called MIMO OTA throughput.

The MIMO OTA throughput is measured at the top of physical layer of LTE and NR system. Therefore, this is also measured at the same point as in the conductive measurement setup: under the use of FRC, the SS transmit fixed-size payload bits to the DUT. The DUT signals back either ACK or NACK to the SS. The SS then records the number of ACKs, the number of NACKs, and the number of DTX TTIs respectively. Hence the MIMO (OTA) throughput can be calculated as

$$MIMO\,(OTA)\,Throughput = \frac{Transmitted\ \ TBS \times Num\ of\ \ ACKs}{Measurement\ \ tTime} \quad (6\text{-}10)$$

where Transmitted TBS is the Transport Block Size transmitted by the SS, which is fixed for a FRC during the measurement period. Measurement Time is the total composed of successful TTIs (ACK), unsuccessful TTIs (NACK) and DTX-TTIs.

The time-averaging is to be taken over a time period sufficiently long to average out the variations due to the fading channel. Therefore, this is also called the average MIMO OTA throughput. The throughput should be measured at a time when eventual start-up transients in the system have evanesced.

The UL/DL port of the radio communication tester is connected to one of the fixed measurement antennas of the chamber. The second DL port of the radio communication tester is connected to the second fixed measurement antenna of the chamber. Other equipment inside the RC, such as the reference antenna and cables, should be terminated with 50 ohm terminations. The RC is loaded to an RMS delay spread of 80 ns using the absorbers.

RC do not offer control over angular distribution and cross polarization discrimination (XPD)

of the channel and would reduce the impact of ECC. The test results in RC are different from those in MPAC or RTS, but the rank is basically consistent. The required measurement distance for RC is half wavelength, thus the chamber size is much smaller than MPAC. The test time of RC is also much less and cut down the total cost

The RC method can be used to measure isotropic metrics like TRP, TRS and MIMO throughput within very short time but it can't provide metrics carrying directional information like antenna pattern, EIRP or EIS.

6.2.5 Reverberation Chamber + Channel Emulation (RC+CE)

The measurement setup for Single/Multiple Carrier Aggregation MIMO TPUT measurements utilizing a reverberation chamber combined with a channel emulator for extending the Channel models.

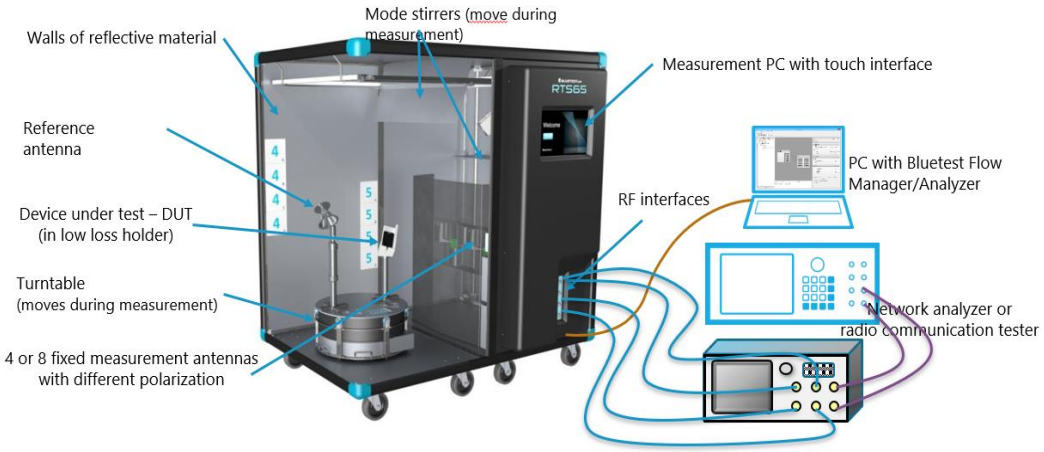

Figure 6-26 Measurement setup for MIMO TPUT measurements, utilizing a reverberation test system combined with a channel emulator.

The following list of equipment is required to perform MIMO TPUT measurements with the RC and channel emulator combination.

- Reverberation chamber
- Radio communication tester
- Channel emulator
- RF cables (2/4 cables connecting the radio communication tester to the channel emulator and 4 cables connecting the channel emulator to the reverberation test system for 2x2/4x4)
- Absorbers (if applicable)
- Applicable DUT holder
- Applicable phantoms (e.g. SAM head phantom, hand phantom or laptop phantom)

The purpose we use RC+CE is to extend the channel models which are not possible implemented in RC standalone setup. But the measurement procedure are same with RC standalone.

The following 3D isotropic model is based on the NIST model with isotropic AoAs and added XPR values and Velocity. The cluster model described below is a simplification of the full model, where a continuous exponential decaying power transfer function with an RMS delay spread of 80 ns is obtained.

Table 6-3 Isotropic model based on the NIST channel model

Cluster #	Delay [ns]	Power [dB]	AoD [°]	AoA [°]
1	0	0.0	N/A	Average isotropic1
2	40	-1.7	N/A	Average isotropic1
3	120	-5.2	N/A	Average isotropic1
4	180	-7.8	N/A	Average isotropic1
5	210	-9.1	N/A	Average isotropic1
6	260	-11.3	N/A	Average isotropic1
7	350	-15.2	N/A	Average isotropic1
Delay spread [ns]				80
Cluster AS AoD / AS AoA [°]				N/A / Average isotropic1
Cluster PAS shape				3D uniform
Total AS AoD / AS AoA [°]				N/A / Average isotropic1
Mobile speed [km/h]				1
XPR2				0 dB

The parameters of the channel models are the expected parameters for the MIMO OTA channel models.

However, the final channel model achieved for different methods could be a combined effect of the chamber and the channel emulator.

The Rayleigh fading may be implementation specific. However, the fading can be considered to be appropriate as long as the statistics of the generated Rayleigh fading are within standard requirement on Rayleigh fading statistics.

7 Evaluation for mmWave 5G Device

7.1 Introduction

5G mmWave devices are quite different with traditional 4G/3G/2G bands since a number of factors contribute to the increasing levels of integration in 5G mmWave devices. These factors are interrelated and are driven by the combination of high frequencies, large numbers of antenna elements, the need to minimize signal path attenuation, and the need to reduce cost. A significant consequence of the resulting integration is that traditional RF connectors at the boundary between the radio distribution network circuit and the antenna system are no longer possible to implement, which means it will not be able to physically expose a front-end cable connector to the test equipment.

As in Figure 7-1, which is an example of mmW UE design. The distribution network employed to connect mmWave signals from the radio to the antenna is extremely compact, especially in handheld devices and other user equipment. As a result, transceiver systems for 5G mmWave devices will be directly integrated with the antenna arrays as shown. In these types of devices, there are no longer connectors or probe points that might enable conducted tests; instead, the great majority of testing must now be accomplished OTA.

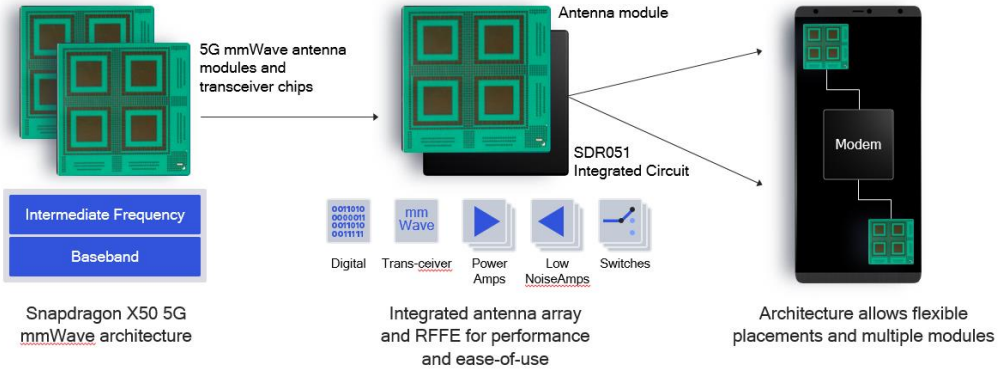

Figure 7-1 mmW UE RF design

The OTA measurement methodologies are typically made in either the radiated near-field or radiated far-field regions of the antenna system under test, as shown in Figure 7-2, where *D* is the diameter of the smallest sphere encapsulating all the radiating elements of the antenna, which may include passive elements. The DUT antenna configuration as defined in Table 7-1 would be tested in UE RF testing. DUT antenna configuration can be chosen by an optional declaration from a manufacturer. And one available test method will have applicability to at least one DUT antenna configurations.

The detailed applicability of any test method for any test will be a function of DUT antenna configuration, the actual testing distance and the resulting calculated MU. If the calculated

MU is lower than the threshold MU, then that test method is applicable to the test.

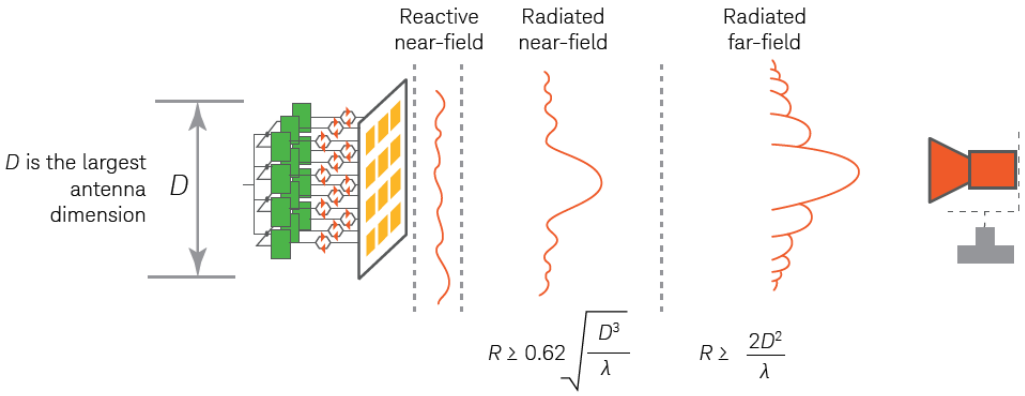

Figure 7-2 Near field and Far field regions for OTA test

Table 7-1 DUT Antenna Configuration

DUT Antenna Configuration	Description
Configuration 1	Maximum one antenna panel with D ⩽ 5 cm active at any one time
Configuration 2	More than one antenna panel D ⩽ 5 cm without phase coherence between panels active at any one time
Configuration 3	Any phase coherent antenna panel of any size (e.g. sparse array)

The RF characteristic of mmWave 5G devices is different from the devices using Sub-6GHz operating band. For example, unlike omnidirectional antennas, the radiation pattern of mmWave array antenna is a high gain directional antenna. The mmWave array antenna used in 5G mobile device is an active phased array. Each antenna of the array is connected with T/R components to realize more flexible beamforming and wide-angle coverage. The example design shown in Figure 7-3 can be used as an example.

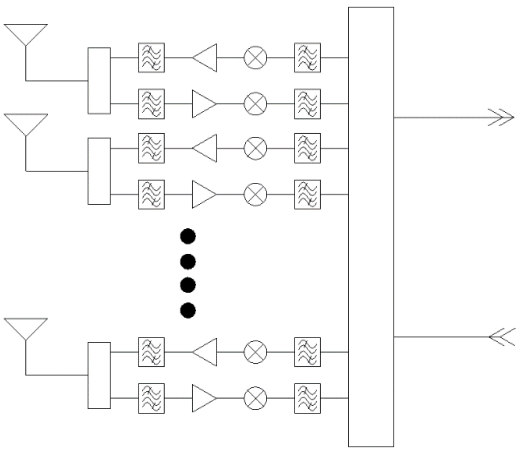

Figure 7-3 Digital phased array for example design

The maximum coverage capability of mmWave 5G device products can be described by EIRP and EIS. As shown in Figure 7-4, the beamforming coverage can be described using a three-dimensional angle.

Note: All of these do not contain polarization effects, only the total energy efficiency is measured.

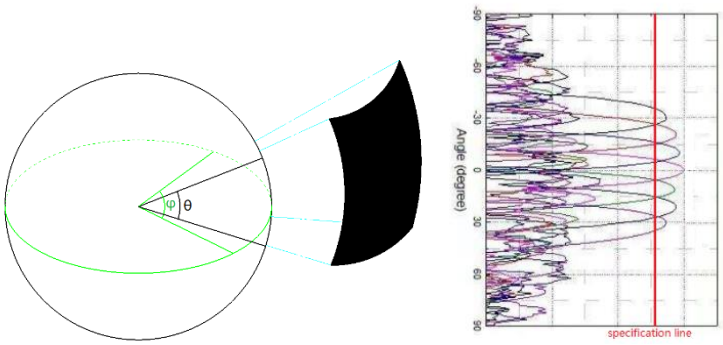

Figure 7-4 Specification in Three-dimensional

The antenna array size shown is ≤36mm*12mm*h, h is the thickness, which value depends on the module implementation process. In this size, 6*2 antennas can be placed @25GHz, 14*4 antennas can be placed @60GHz. At the same time, in theory, the former can get the highest array gain of 10dB, and the latter can get 17.3dB.

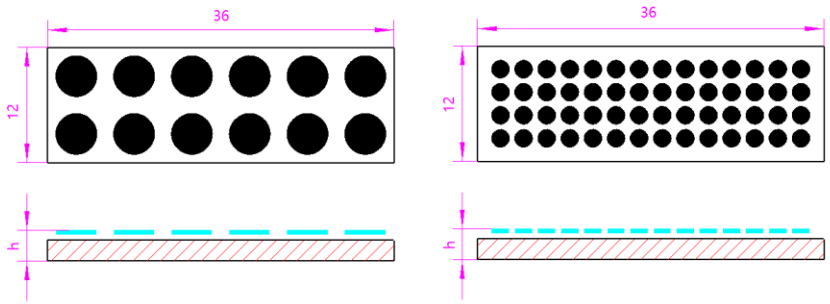

Figure 7-5 Array Schematic Diagram

On the other hand, we have known that electromagnetic waves have weak ability to diffract around obstacles with a size significantly larger than the wavelength. Therefore, mmWave communications are sensitive to blockage by obstacles such as building, foliage and body. For example, blockage by a human penalizes the link budget by 20-30 dB. The blockage loss has a big impact on the RF performance. To overcome the impact of blockage, diversity can be considered to apply in mmWave communication. The following two figures show how to leverage path and UE diversity to overcome blockage in mmWave.

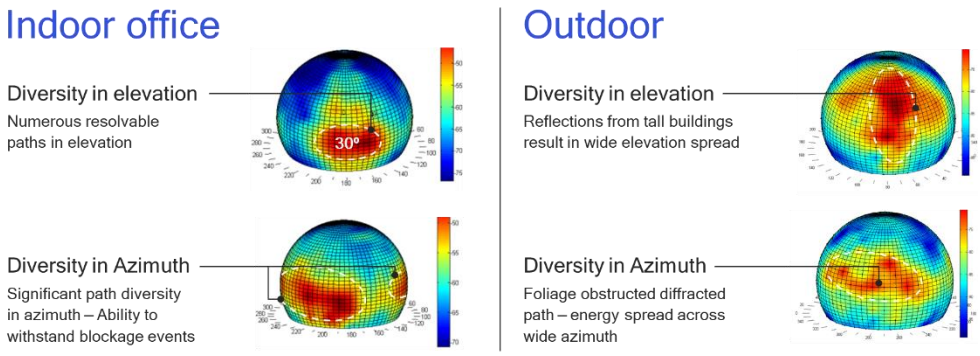

Figure 7-6 Leverage path diversity to overcome blockage

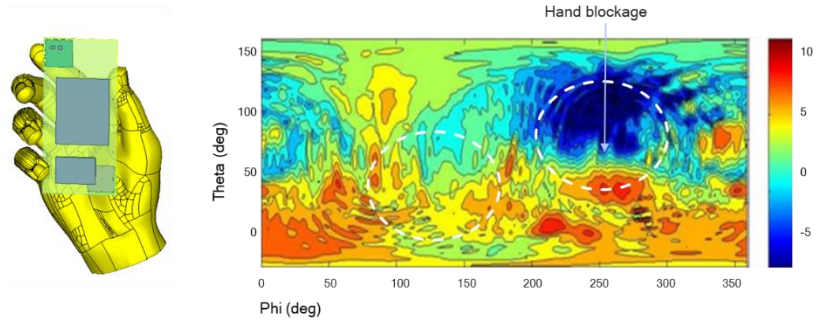

Figure 7-7 Leverage UE antenna diversity to overcome hand-blocking

For mmWave 5G device RF performance, all the requirements including EIRP, EIRP spherical coverage, TRP, EIS, EIS spherical coverage, EVM, spurious emissions and blocking metrics, etc. defined in TS38.101 should be tested based on OTA methodology.

7.2 RF test methods

7.2.1 Direct Far Field (DFF)

7.2.1.1 Introduction of far-field

A common direct far field (DFF) measurement setup of UE is shown in the Figure 7-8.

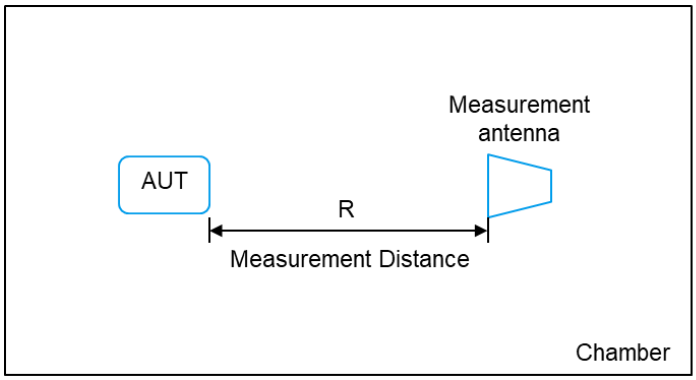

Figure 7-8 DFF measurement setup of UE

The minimum far-field distance (R) for a traditional far field anechoic chamber can be calculated based on Fraunhofer distance (FHD) criterion ($R = 2D^2/\lambda$), where D is the diameter of the smallest sphere that encloses the radiating parts of the DUT, and λ represents the wave length.

Far-field (FF) is generally considered to start at the Fraunhofer distance. This criterion may however be overly conservative when the antenna occupies a very small volume of the radiating equipment. This case will exactly happen with mobile devices operating 5G New Radio (NR) at frequencies in the 28 and 39 GHz ranges. Normally for a UE device, the typical antenna aperture size for 5G handsets, chipset and mobile phone vendors is smaller than a couple of cm size. Although the device size could be for example 15 cm for a typical mobile phone or larger.

Indeed, the antenna size of the 5G NR device is normally smaller than 5 cm. For example, for a 2cm-sized antenna array, RHD gives a FF distance of 8 cm at 28 GHz. For a 15cm-long mobile device, applying D=15 cm results in a FF distance of 4.2 m. Actual devices are however not completely covered with antenna arrays and the 2-cm antennas are made to essentially operate as standalone radiating elements. The FF behavior must hence start in space at a much shorter distance than 4.2 m. In 3GPP TR 38.810, the device under test (DUT) is first classified into three categories.

The following table (Table 7-2) describes method applicability of permitted test methods for DUTs in different categories.

Table 7-2 Overview of test method applicability for permitted test methods

DUT category	Direct Far Field (DFF)	Indirect Far Field (IFF)
Category 1	Yes	Yes
Category 2	Yes	Yes
Category 3	No	Yes

In other words, for the DUT classified in the Category 1 and 2, the DUT vendor or manufacturer requires the exact location of the antenna array to characterize the antenna and the antenna on chip performance, e.g. the beamforming parameters. Actually, the knowledge of a precise antenna location is quite critical for the design and the adjustment for the R&D propose. However, the measurement of the DUT of Category 3 pays more attention to the performance of the whole device. The antenna location could be unknown during in case, which is usually called black box method. Thus, a quite zone >5 cm is required.

According to the far-field criteria, the far-field distance and the corresponding path loss could be calculated as shown in the table 7-3.

Table 7-3 Near field/far field boundary for different frequencies and antenna sizes for a traditional far field anechoic chamber

D(cm)	Frequenc y (GHz)	Near/far boundary	Path Loss(dB)	Frequenc y (GHz)	Near/far boundary	Path Loss(dB)

		(cm)			(cm)	
5	28	47	54.8	100	167	76.9
10	28	187	66.8	100	667	88.9
15	28	420	73.9	100	1501	96
20	28	747	78.9	100	2668	101
25	28	1167	82.7	100	4169	105
30	28	1681	85.9	100	6004	108

As shown in the table above, a DFF distance of 47 cm leads to a Far field path loss of 54.8 dB considering a radiating size D of 5 cm. This value rises rapidly with the corresponding D. This could result to a large and expensive chamber. Also, the path loss increases with the operation. As shown in the table, DFF distance of 167 cm at 100 GHz leads to a path loss of 76.9dB. Large distance causes high path loss which has influence on the system's dynamic range. Especially in the 5G NR millimeter-wave range, the dynamic range of the OTA system is quite limited due to the high path loss.

There is thus some studies on the far- field measurement in a shorter test distance compared with FHD. Actually, an experimental method was proposed to determine the far field distance based on path loss measurements. This method is based on the fact that the path loss exponent is different in the near field and the far field. A recent publication, has introduced novel theoretical results showing that the actual FF behavior in the peak directivity region can start at a distance much shorter than the FHD. As a result, the FF EIRP or EIS of a 15 cm DUT can be assessed at a distance of 30% of the FHD. It should be mentioned that this short distance is enough to access the main beam of the radiation pattern. However the FHD allows a lower errors in side lobe pattern measurements.

7.2.1.2 Calibration of far-field

The calibration measurement is done by using a reference antenna with known gain values. The path loss could be measured in the following setup (Figure 7-9).

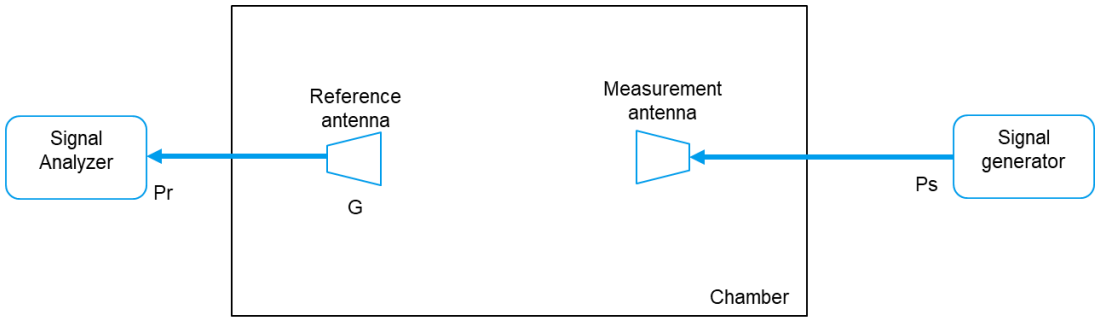

Figure 7-9 Calibration process of the DFF measurement setup

The path loss could be calculated as:

$$PL = G + Pr - Ps \quad (7\text{-}1)$$

Where, G stands for the gain of the reference antenna; Ps and Pr represent the output power of the signal generator and the input power to the signal analyzer. Thus, the calibration process determines the composite loss of the entire transmission and receiver chain path gains (measurement antenna, amplification) and losses (switches, combiners, cables, path loss, etc.). The calibration measurement should be repeated for each measurement path (two orthogonal polarizations and each signal path).

7.2.2 Compact Antenna Test Range (CATR)

IFF methods creates far field environment using transformation method. There are several different kinds of technologies to create far field environment, for example Plane Wave Synthesis, reflector, etc. This section introduces a method creating the far field environment using a transformation with a parabolic reflector. This is also known as the compact antenna test range (CATR).

The IFF measurement setup of CATR is shown as Figure 7-10. CATR system adopts the reflector to transform spherical wave to plane wave in the desired quiet zone. A CATR Range is a geometrical optical design and reciprocal, they support device measurement in both transmit and receive measurement. This method has been accepted by 3GPP as a standardized test method in 3GPP TR 37.84 for Active Antenna System (AAS) Base Station (BS) RF measurement and 3GPP TR 38.810 for 5G UE RF measurement. CATR solution can work with all frequencies defined for FR2.

The key aspects of this test method setup include reflector, position/rotation system, measurement probe antenna and link antennas.

The reflector design is one of the key point for CATR implementation and edges diffraction needs to be minimized using edge treatment. Two common edge treatments are: Serrated edge and Rolled edge. With serrations edge design there is a smooth transition between parabolic surface of the reflector and free space, thus reducing the diffraction effects and directing the diffracted field away from the quiet zone. The length of serrations defines the lowest operation frequency, typical serrations length is 5 times wavelength. Rolled edge is designed as that the edges of reflector are smoothly bent backwards thus reducing the energy at the edges of the reflector.

The position/rotation system can adjust the angle between dual-polarized measurement antenna and DUT, it at least needs support two axes of rotation freedom. In the CATR system positioner is placed in the quiet zone where the DUT is. The size of the quiet zone determines the maximum DUT size, which is restricted by the reflector size.

The measurement antenna is placed in a proper position in chamber to feed the test signal to reflector and then to the quiet zone for transmitter test, receive the signal from the DUT to reflector and then to feed antenna for receiver test. Link antenna is equipped to allow the 3D radiation pattern test when do UE beam lock test. If no beam lock function is tested the measurement probe antenna works as a link antenna to maintain the connection. Once the

beam is locked the link is to be passed to the link antenna which maintains reliable signal level with respect to the DUT. Then the DUT can be rotated to measure the 3D radiation pattern without losing the connection with the BS emulator.

One benefit from CATR compared with Direct Far Field is that it can shorten the test distance and lower the path loss while still satisfy the Far Field test criteria. We know large dynamic range is one essential requirement for OTA test, especially for mm wave frequency test. Large path loss will bring big challenges for measurement dynamic range. Then CATR test environment with lower path loss will have larger measurement dynamic range compared with Direct Far Field.

According to the specification in TR38.810, the applicability criteria of this test method are:

- The total test volume is a cylinder with diameter d and height h
- DUT must fit within the total test volume for the entire duration of the test
- Either a single radiating aperture, multiple non-coherent apertures or multiple coherent apertures DUTs can be tested.
- EIRP, TRP, EIS, EVM, spurious emissions and blocking metrics can be tested.
- No manufacturer declaration is needed

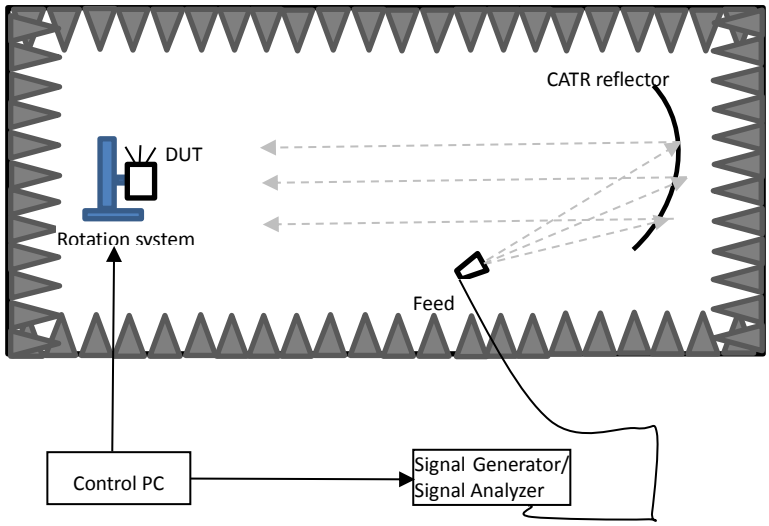

Figure 7-10 IFF method 1 (CATR) measurement setup of UE RF characteristic

7.2.3 Conical Compact Range

Conical compact range antenna means to combine the traditional CATR and robotic arm to approach the far-field antenna measurement. Due to in the 5G MMW measurement the problem of SDO (suspect disturbing objects) will influence more than the traditional 3G or 4G measurement. With the helping of the robotic arm, it can decrease the total area which exposed in the measurement environment and can set up different measurement ways easily (Spherical, UV, planar…). Just need to advise the software system and adjust the gesture of the robotic arm.

The reason why SDO problem is so important in the 5G mmW measurement is that the gain of the MA and DUT are very high in the high frequency, which are about 20~30db and it may cause high reflection power to influence the antenna gain, direction, phase and null point measurement.

The formula of the SDO is as following

$$SDO=G_{DUT}G_{MA}\left(\frac{\lambda}{4\pi r_2}\right)^2\left[\frac{\sigma}{4\pi r_1^{\,2}}\right] \quad (7\text{-}5)$$

Where：

r_1= the distance between SDO and MA

r_2= the distance between SDO and DUT

σ = the bistatic scattering cross section of SDO

G_{DUT} = The gain of the device under test

G_{MA} = The gain of the measurement antenna

It is noted that in order to perform the great circle cut measurement, a strong holder to support the DUT/AUT is required. In particular, at mmW frequencies low dielectric constant material is required, which, however, cannot provide strong mechanical structure. Furthermore, in the past 3G cellphone test, the gain of DUT and CRA is roughly 0 ~ -3db. However, in the mmW system, the gains of DUT and CRA are very high for at least 20~30db which may cause high reflection power to influence the antenna gain, direction, phase and null point measurement. As a result, the test system is developed to perform the conical-cut measurement by using a robot arm to control ψ and θ rotation from outside. As a result, the DUT does not need strong mechanical structure to perform the ψ rotation by robot arm. The test system can then use low dielectric constant material to reduce the scattering power of interference. As a result, the test system is developed to perform the conical-cut measurement by using a robot arm to control ψ and θ rotation from outside. so, the DUT does not need strong mechanical structure to perform the ψ rotation by robot arm. The test system can then use low dielectric constant material to reduce the scattering power of interference.

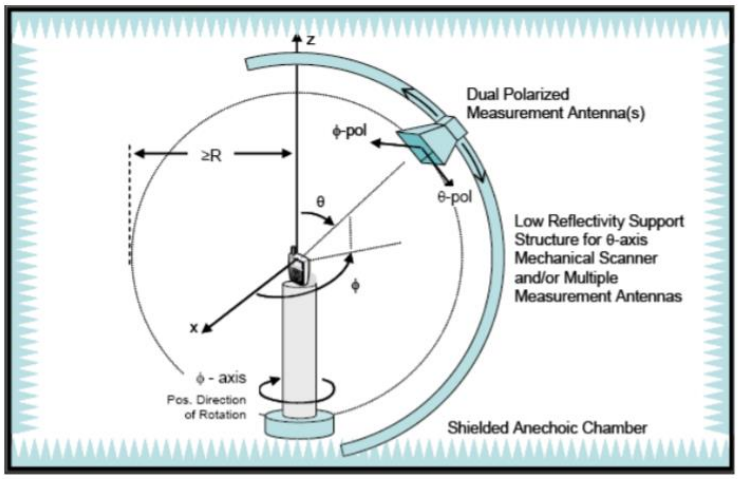

Figure 7-11 Conical cut way

The major feature of this system is that the AUT/DUT doesn't need to move when it under the test, all the movement of the AUT or MA are replacing by the robotic arm. It means that the measurement result can be more stable and useful, decreasing the possibility of the phase error.

Furthermore it can finish the measurement in the short time, due to the robotic arm can change the rotate center easily, it can adjust the north pole due to the AUT may not arrange on the proper place like Figure 7-12

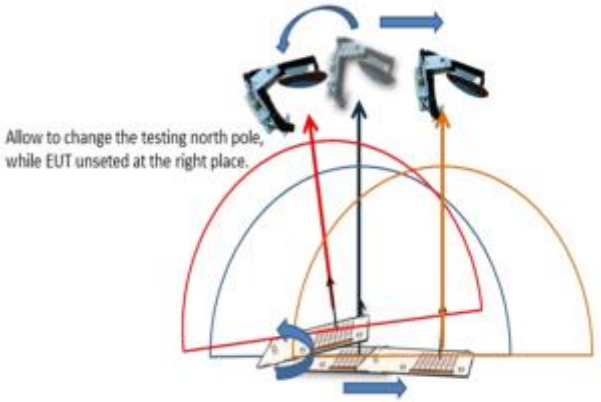

Figure 7-12 Adjust the robotic arm which based on different arrangement of the AUT

Third, by the software and the LSF algorithm helps, after few times of the xy plane scanning , the system can make sure the rotate center and the phase center of the antenna is on the same place as Figure 7-13 which indicates the problem that the center of rotation is not overlap to the phase center of antenna.

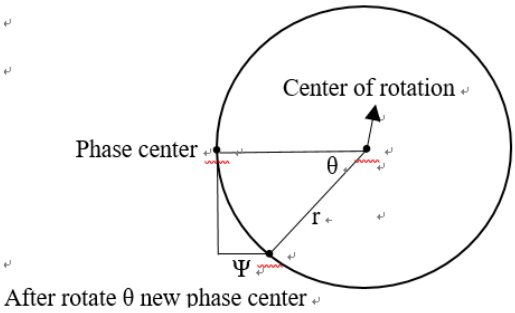

Figure 7-13 Phase center and rotate center are not on the same place

Base on the formula

$$r = \frac{\lambda}{2\pi}\left(\frac{\Psi}{1-\cos\theta}\right) \tag{7-6}$$

Where

r = the radius between phase center and rotate center

λ = the antenna wavelength

Ψ= the phase change when rotate θ

θ = the rotate degrees

The system needs to adjust the Ψ variation to minimize the r toward 0. In the conventional method, even the conical cut measurement of CTIA specification still need to do the phase center measurement based on the IEEE 149std. It will need precise positioning and minimum mechanical tolerances in the positioner. Furthermore, it needs more complex mechanical structures, where the SDO problem mentioned above will happen

Fourth, the system can move 0.1 degree per step, make the measurement more precise, as the Figure 7-14

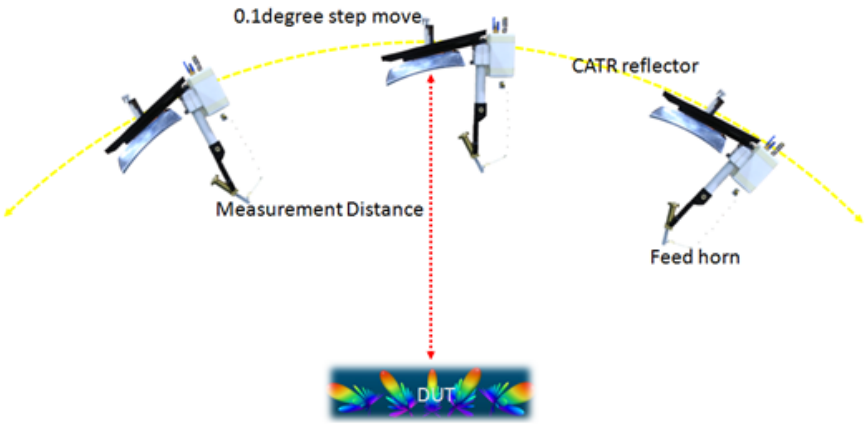

Figure 7-14 The minimum degree per step

The system arrangement will as Figure 7-15 Conical-Cut Radiation CATR Measurement, to make the whole system in the chamber and uses the SG to open the mixer, by the particular up/down converter to extend the bandwidth of the measurement, make the system more flexible and usable, also it decreases the fee of the instrument.

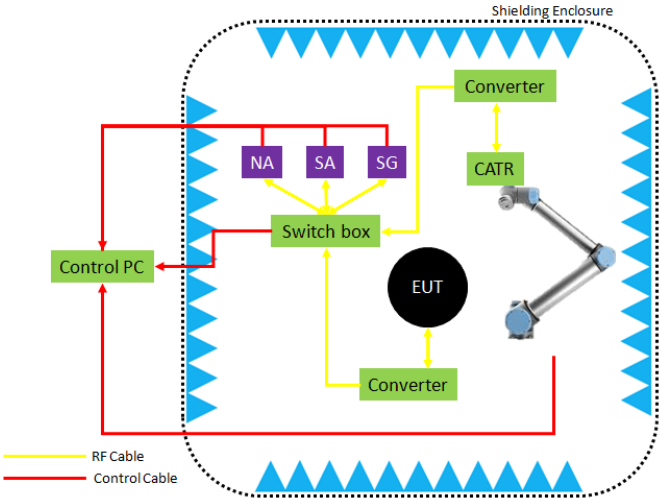

Figure 7-15 Conical-Cut Radiation CATR Measurement

The methods to set up are :

- Let the distance between AUT and CATR follow the 3GPP agreement
- Use the x-y scanning to find the coordinate of the antenna phase center(LSF way to convergence)
- Use that coordinate as the central point of the conical cut measurement
- Start to measure the 3D.Phase.amplitude.TRP.EIRP.EIS
- Use the software to compensate the path loss
- Use the software to adjust the distance between the AUT and CATR

Method improve amplitude and phase error

The system adjust the distance between the AUT and MA based on this formula, in order to improve the amplitude and phase error.

$$\Delta Z = \frac{1}{2\sin\theta_0}\frac{\varphi(-\theta_0)-\varphi(\theta_0)}{2\pi}\lambda_0 \qquad (7\text{-}7)$$

Where：

z = rotate robotic arm with this new radius

θ_0= the robotic arm rotate angle

λ_0= the wavelength of free space

$(-\ \theta_0)$ and (θ_0) are the symmetrical angles$\pm\theta_0$ phase angle

As a result the software of the system can adjust the robotic arm rotate radius based on this formula, △z will be the new radius of the robotic arm.

7.2.4 Near Field to Far Field Transform (NFTF)

7.2.4.1 NFTF techniques

The near field to far field transformation is based on the measurement of the amplitude and phase of the signal radiated by the Device-under-test (DUT) on a defined surface (planar, cylindrical, spherical) in the near field region. The complex signal is detected by a probe that is moved along the selected surface type. By applying probe calibration techniques, the influence of the probe on the measured signal may be corrected. In particular, the data collected from all measurement points on the whole surface represents the input to numerical techniques that are able to evaluate the transmission properties of the DUT. The SWE (Spherical wave expansion) is the relevant method for spherical NF surfaces; once it is applied, the field radiated by the DUT can be computed at any distance; the far-field pattern can be also evaluated.

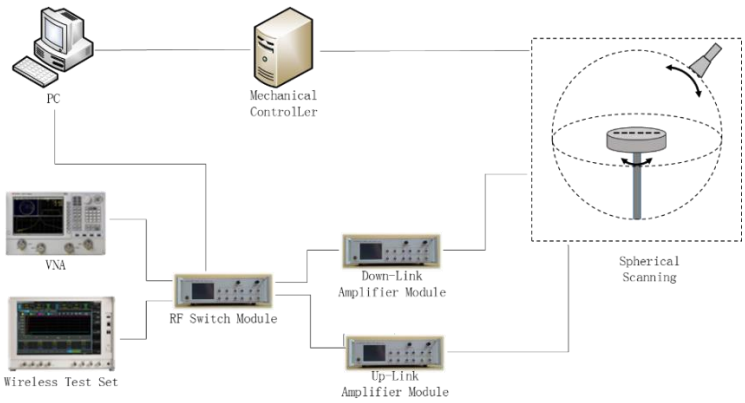

Figure 7-16 Baseline setup of NFTF

7.2.4.2 Probe Calibration

An accurate application of the NF to FF transformation techniques requires the precise knowledge of the probe characteristics; the probe does not measure directly the radiated field but a weighted average of the field present on the probe aperture. The knowledge of how this field is transformed into the signal received at the probe load is expressed in terms of the probe receiving coefficients $R^{(p)}$. Therefore $R^{(p)}$ should be known before the SWE technique may be applied. This task is accomplished by a probe calibration procedure to be applied in advance for each specific probe of interest.

7.2.4.3 Obtaining phase

The knowledge of both amplitude and phase of the probe complex signal is crucial for reliably applying the NF to FF transformation techniques. Although the Vector Network Analyzer (VNA) is the more suitable instrument for NF antenna measurements since it detects both the signal amplitude and phase, it may not always employed, especially when complex and highly integrated antenna array systems are tested. Therefore only the signal amplitude is directly measured. The signal phase needs to be recovered by additional steps. The main technique to achieve this goal relies on the detection of the signal amplitude on two different NF surfaces at appropriate distance from each other; then an iteration process is applied, together to an initial estimation value of the phase.

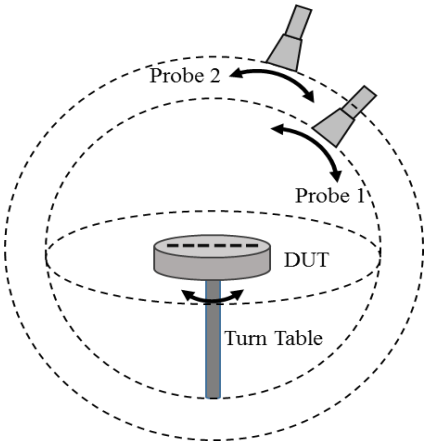

Figure 7-17 Spherical scanning

7.2.5 Near Field without Far Field Transform (NFWOTF)

Considering the UE RF test cases in FR2 with low power spectrum density, such as OFF power/Tx spurious/Rx spurious, with the path-loss, thermal noise and an actually-attainable NF (noise figure) of a power measurement equipment, the power densities are too low to be measured directly in the DFF measurement setup, which imposes on us the necessity to think of another permitted measurement setup. This is the background to introduce NFWOTF.

The baselines which NFWOTF would reply on include:

As long as TRP measurements are concerned, the measurements can be performed in the **radiative near-field region** (outside the reactive near-field region), because the total radiated power through the whole sphere area does not depend on the distance between the DUT and the measurement antenna. Based on this idea, it would be possible to measure TRP in radiative near-field without the near-field to far-field transform, which is useful in such situations where the signals to be measured cannot be replaced with CWs, because the near-field to far-field transform shall be difficult without using CWs.

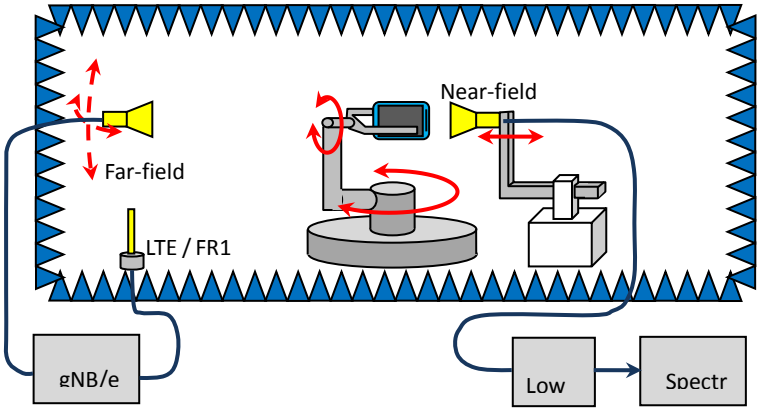

Figure 7-18 NFWOTF measurement setup of UE RF characteristics

By adjusting the distance between the DUT and the measurement antenna so that the radiative near-field criteria and the condition to sample the DUT-radiation pattern independently enough are met while keeping the distance as short as possible, it would be possible to curtail the large path-loss in mmWave, which is beneficial to secure a good SNR condition.

The image of NFWOTF setup is shown in Figure 7-18, and the key aspect of the NFWOTF setup are:

- Radiative near-field measurement system in an anechoic chamber
- A dual-polarized measurement antenna placed in the radiative near-field region from the DUT
- A link antenna for NR connections placed in the far-field region from the DUT
- A positioning system such that the angle between the dual-polarized measurement antenna and the DUT has at least two axes of freedom and the distance between the dual-polarized measurement antenna and the DUT is adjustable
- A positioning system such that the angle between the link antenna and the DUT has at least two axes of freedom and maintains a polarization reference; this positioning system for the link antenna may or may not provide independent control from the measurement antenna.

Regarding to Calibration in NFWOTF, even without knowing the gain value of the calibration antenna in the radiative near-field region, the calibration can be performed by comparing the measured TRP with the radiation power calculated by the power fed to the reference antenna through the cable and the radiation efficiency.

Following Table 7-4 and 7-5 showed comparison between NFM without Near-to-Far Transform and DFF. Even the lowest TRP levels in UE RF test cases can be measured in NFWOTF setup with the SNR as well as 7.9dB, assuming the measurement antenna gain of 10dB, the NF of

10dB, Device size=15cm, while the same lowest TRP levels can't be measured directly in DFF setup having -4.2dB SNR in 43.5GHz.

Table 7-4 SNR and Power deviation with NFM without Near-to-Far Transform method

Frequency [GHz]	$\frac{\lambda}{2\pi}$ [m]	Min. Radiative NF distance [m]	Centre of rotation to Meas.Ant distance [m]	Path-loss [dB]	Meas. Ant. gain [dBi]	Target Level [dBm/Hz]	SNR [dB]	Power deviation due to SNR [dB]
1.0	0.0477	1.153	1.228	34.2	10.0	-107.0	32.8	0.00
6.0	0.0080	0.192	0.267	36.5	10.0	-107.0	30.5	0.00
24.0	0.0020	0.048	0.123	41.8	10.0	-120.8	11.4	0.31
43.5	0.0011	0.027	0.102	45.3	10.0	-120.8	7.9	0.66
87.0	0.0005	0.013	0.088	50.1	10.0	-107.0	16.9	0.09
45.5	0.0011	0.027	0.225	52.3	14.70	-120.8	5.6	1.05

Table 7-5 SNR and Power deviation with DFF method

Frequency [GHz]	2*D^2/ lambda [m]	Path-loss [dB]	Target Level [dBm/Hz]	SNR [dB]	Power deviation due to SNR [dB]
1.0	4.639	45.8	-107.0	26.2	0.01
6.0	1.186	49.5	-107.0	22.5	0.02
24.0	0.400	52.1	-120.8	6.1	0.95
43.5	0.725	62.4	-120.8	-4.2	5.61
87.0	1.450	74.5	-107.0	-2.5	4.41

7.3 RRM test methods

Here two test methods are proposed, method 1 has been included in 3GPP TR 38.810 for R15 RRM test, method 2 is a simplified MPAC method which has the ability to generate adaptive signal distribution.

7.3.1 Method 1

The baseline measurement setup of UE RRM characteristics for frequency bands above 6GHz can establish an OTA link between the DUT and a number of emulated gNB sources and is shown in Figure 7-19, this is a suggested setup from TR 38.810 for UE RRM test.

The key aspects of this test method setup include dual-polarized probe antennas, position/rotation system. If multiple probe antenna system is equipped, switch system is required to distribute the downlink signals from gNB to different probe antennas dynamically to emulate the different angles of the arrival.

It is supposed that multiple emulating signals can be simultaneously active. The position/rotation system can provide angular relationship with two axes of freedom between the DUT and the test systems.

For the propagation conditions it is suggested multi-path fading propagation is emulated between the DUT and the emulated gNB, but this test setup cannot emulate accurate spatial channel model, only emulate the effect of signal direction change.

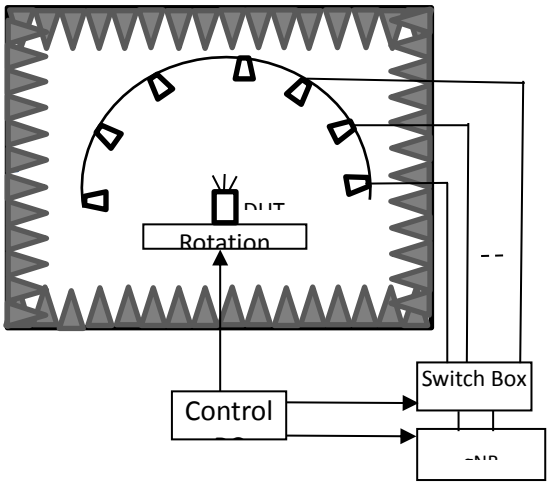

Figure 7-19 Baseline measurement setup of RRM characteristics

7.3.2 Method 2

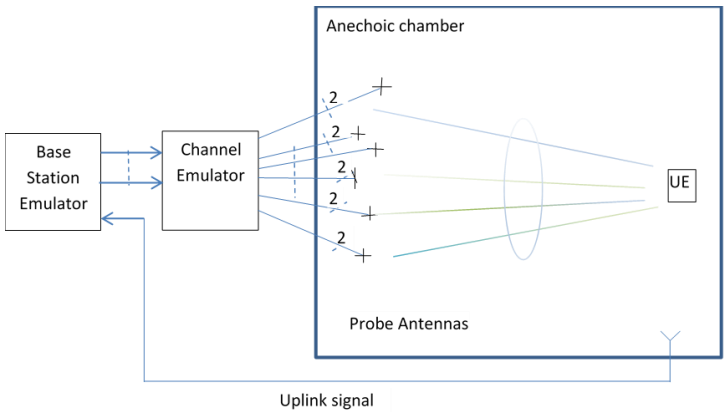

Figure 7-20 Simplified Sectorized MPAC (SS-MPAC) setup for RRM and demodulation test

Another suggested method to test RRM is Simplified Sectorized MPAC (SS-MPAC) shown in above figure. Given the MPAC method is well accepted for 4G UE MIMO OTA test, it is straightforward to think about extending the MPAC method to mmWave applications. However, the direct extension to three a dimensional channel model and application to mmWave appears impractical because too many probe antennas are required when the wavelength decreases and the size of the DUT increases. The significantly increased system complexity comes from two aspects: the probes themselves and the channel emulator connected to the probes. The SS-MPAC method is proposed to solve these two issues. Figuer 8-20 shows SS-MPAC setup for

illustration. The probes are installed in the form of a sector of angles with approximately equal distance R from UE and with certain angular spacing. One of the enablers for the cost effective sectorized MPAC testing is the observation of small cluster Angular Spread (AS) at mmWave and the beamforming performed at the Tx and Rx ends, which filters out, effectively weak multipath clusters of the channel model. Another enabler is to use switching circuitry between the channel emulator and probe antennas. This means that the number of installed probes in the sector is significantly higher than the number of active probes used to reproduce the channel model in the chamber. In this way the total cost of the test system is lowered by removing the requirement for the number of emulated channels, while the capability to reproduce realistic and dynamic channel models is preserved because of the freedom to select active probes. For SS-MPAC methods, far-field is assumed for the test process.

7.4 Demodulation test methods

Being similar with RRM testing, in demodulation testing, all components which operate at the radio frequency such as RF filters, duplexers, transmit receive switch, low noise amplifier (LNA), power amplifier (PA), analogue beamforming phase shifting elements etc., and the algorithms which control such components from the test should be considered. Moreover, the details on how to control SNR of DL signal at reference point etc. should be defined in the demodulation testing.

For a Near-Field setup the reference point for SNR of DL signal is defined as the intersection of the axes of rotation of the positioning system(s). For a Far-Field (DFF or IFF) setup the reference point for SNR of DL signal is defined as the geometrical center of the QZ. From the UE perspective the reference point is the input of UE antenna array.

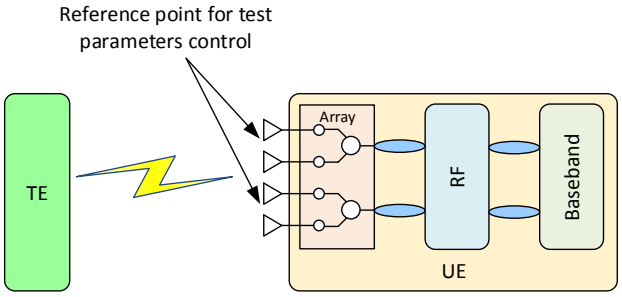

Figure 7-21 DL SNR reference point for UE Demodulation and CSI testing methodology

7.4.1 Method 1

Method 1 of RTS with no antenna pattern, includes the RF front end but ignores the impact of the antenna. If it is decided the demodulation requirements mainly focus on baseband performance under any non-spatial tapped delay line (TDL) channel model, method 1 is a good choice. Pre-defined correlation levels or using assumed antenna patterns is also possible.

Method 1 still can use setup shown in previous RTS for up to two streams demodulation test. If the test cases are desired for more than 2 streams, more dual-polarized probe antenna are

required to be installed in the chamber. It is implemented as the 2nd stage of RTS, including inverse matrix tuning and throughput test process.

This method has been approved by 3GPP TR38.810 for R15 UE FR2 demodulation test, named as wireless cable. In TR38.810 it is supposed that using different polarization to generate wireless cable effect directly. This is true if the UE Rx antenna is designed with very good orthogonal polarization diversity, and maximum tested stream number is two. If the test cases include larger than two streams, or the UE Rx antenna does not have so realistic polarization diversity, inverse matrix tuning and implementation is mandatory in the whole test procedure.

7.4.2 Method 2

Method 2 of RTS with the antenna pattern, resolves the issues with method 1 regarding the importance of the antenna pattern. Its hardware complexity is the same as method 1 and all that is required is the measurement of the pattern which can be reused for many different demodulation requirements. It is therefore expected there would be no meaningful increase in test time or test cost over method 1 while providing a much more comprehensive measure of the UE performance. The main issue with method 2 is whether it is possible to get the UE into a condition where the correct antenna pattern is selected by the UE for the channel model to be applied. Method 2 can use the same setup as method 1.

7.4.3 Method 3

As was the case with LTE MIMO OTA, the multi-probe anechoic chamber (MPAC) test method had the fewest restrictions although it came with the highest cost/complexity. It doesn't need a UE test mode to measure the antenna pattern, it isn't restricted by the number of UE receivers and can handle dynamic antenna patterns in response to the applied channel model (be the static or dynamic) There is some increase cost/complexity with the SS-MPAC system although the number of active probes is expected depend on the channel model.

Method 3 using spatial emulation is the only method that can address the general case for arbitrary UE beamforming. This method is also capable of testing the dynamic performance of the UE's antenna system with the emulation of dynamic geometry channels which will be typical of any realistic deployment.

The main open issue with Method 3 is the ability to emulate the channel with sufficient control over the spatial correlation when testing large aperture directive DUT antenna systems. For LTE MIMO OTA test 2D spatial channel model is emulated and signal spatial spread for UE on sub-6 GHz is large. When move to 5G mm Wave UE test, 3D channel model emulation is required and signal spatial spread turns to be significantly narrow, the channel characters emulation brings the new challenges for this method: how far the multiple probe antennas should be positioned and how much active probe antenna is enough to emulate the 3D spatial channel model accurately.

The method 3 can use the setup in 7.3.2, this setup is valid for both RRM and demodulation test.

8 References

The following documents contain provisions which, through reference in this text, constitute provisions of the present document.

[1] 3GPP TR 38.810 V2.0.0, “Technical Specification Group Radio Access Network; Study on test methods for New Radio; (Release 15)”, Mar. 2018

[2] 3GPP, TR 38.901, Study on channel model for frequencies from 0.5 to 100 GHz.

[3] 3GPP TR.37.977, “Verification of radiated multi-antenna reception performance of User Equipment (UE)”

[4] Ya Jing, Xu Zhao, Hongwei Kong, Steve Duffy, and Moray Rumney, “Two-Stage Over-the-Air (OTA) Test Method for LTE MIMO Device Performance Evaluation”, International Journal of Antennas and Propagation, Vol. 2012

[5] 3GPP TR 36.978, “Evolved Universal Terrestrial Radio Access (E-UTRA) User Equipment (UE) antenna test function definition for two-stage Multiple Input Multiple Output (MIMO) Over The Air (OTA) test method”

[6] 3GPP TR 37.842: “Radio Frequency (RF) requirement background for Active Antenna System (AAS) Base Station (BS)”

[7] R4-1705838, “Simplified sectorized MPAC for RRM/ Demodulation Setup”, Keysight, RAN4 #83, May 2017

[8] R4-170669, “SS MPAC for RRM/Demod”, Keysight, RAN4 AH#2, June 2017

[10]R4-1711497, “Demodulation and RRM requirements and test scope,” Keysight Technologies, 3GPP RAN4 #84bis, October 2017

[9] R4-1710389 Intel Corporation “On demodulation baseline system”

[10] R4-1708996, “WF on RRM/Demod baseline test system,” Rohde & Schwarz, 3GPP RAN4 #84, August 2017

[11] R4-1705838,“Simplified sectorized MPAC for RRM/ Demodulation Setup”, Keysight, RAN4 #83, May 2017

[12] K. T. Selvan, R. Janaswamy, “Fraunhofer and Fresnel distances,” IEEE Antennas Propagat. Magazine, Aug. 2017.

[13] B. Derat, “5G antenna characterization in the FF,” Proc. Int. Symp. EMC & Asia-Pacific Symp. EMC (APEMC), Singpore, May 2018.

[14] S. Singh, F. Ziliotto, U. Madhow, E. M. Belding, and M. Rodwell, “Blockage and directivity in 60 GHz wireless personal area networks:From cross-layer model to multi hop MAC design,”

IEEE J. Sel. Areas Commun., vol. 27, no. 8, pp. 1400–1413, Oct. 2009.

[15] Michael D. Foegelle. “Antenna Pattern Measurement: Concepts and Techniques.”

[16] IEEE 10.1109/ISEMC.2018.8393803

[17] CTIA (2015, May). “Method of Measurement for Radiated RF Power and Receiver Performance”, Test Plan for Mobile Station Over the Air performance Rev3.4.2,pp.238-239.Avalible:https://www.ctia.org/docs/default-source/default

[18] The Institute of Electrical and Electronics Engineers. Inc, “IEEE Standard Test Procedures for Antennas”, December 19. 1979, pp. 69-75

[19] RP-010680. TSG-RAN Meeting #13, Beijing, China, September 200,1, pp.18-21

[20] Moray Rumeny, Hongwei Kong, Ya Jing, etc, ‘Recent advances in the radiated two-stage MIMO OTA test method and its value for antenna design optimization’, Conference: The 10th European Conference on Antennas and Propagation (EuCAP 2016)

[21] M.T. Dao, V.A. Nguyen, Y.T. Im, S.O. Park, and G. Yoon,”3D Polarized Channel Modeling and Performance Comparison of MIMO Antenna Configurations With Different Polarizations,” IEEE Transactions on Antenna and Propagation, VOL. 59, NO. 7, July 2011, pp.2672-2682.

[22] 3GPP R4-157298, Keysight Technologies, General Test Technologies, Analysis of AC methodology results